

TECHNISCHE HOOGESCHOOL DELFT  
VLIETUIGBOUWKUNDE  
BIBLIOTHEEK

7 FEB. 1964

CoA. Report Aero No. 165

TECHNISCHE UNIVERSITEIT DELFT  
Luchtvaart- en Ruimtevaarttechniek  
BIBLIOTHEEK  
Kluyverweg 1 - 2629 HS DELFT



THE COLLEGE OF AERONAUTICS  
CRANFIELD

ON THE FLOW IN THE NOZZLE OF A CONDENSING DIATOMIC VAPOUR

by

D. R. Clark

THE COLLEGE OF AERONAUTICS

CRANFIELD

On the Flow in the Nozzle of a Condensing Diatomic Vapour

- by -

D. R. Clark, D.C. Ae.\*

SUMMARY

An investigation is made of the supersaturation and condensation of a pure diatomic vapour in a hypersonic nozzle. The concept of critical droplet size and the theory of spontaneous nucleation are discussed, making allowance for the variation of surface tension with droplet size. In addition, the one dimensional equations for the flow of a condensing vapour are derived and with these equations a satisfactory theory for condensing flows is obtained.

A systematic investigation into the effect of reservoir conditions and nozzle geometry is made. It is found that, in general, increasing the reservoir temperature and reducing the reservoir pressure increases the possible supercooling, while increasing the nozzle length or throat area reduces it. The nozzle static temperature gradient is shown to be an important parameter in the collapse of the supersaturated state. A maximum supercooling of  $16\text{ K}^{\circ}$  is obtained with a nozzle of 0.01 sq. in. throat area and an expansion angle of  $15^{\circ}$  at a reservoir pressure of 8.3atm. and temperature of  $290\text{ K}^{\circ}$ . Agreement with experiment is generally good.

It is found that when a supersaturated vapour is passed into a parallel duct before nucleation is established, a considerable supersaturation can be sustained.

\* This paper is based on work performed in partial fulfilment of the requirements for the Diploma of the College of Aeronautics.

## CONTENTS

	<u>Page</u>
Summary	
List of Symbols	
Acknowledgements	
1. Introduction	1
2. The mechanics of condensation	3
2.1 Drop distribution	4
2.2 Rate of formation of nuclei	4
2.3 The effect of droplet size on surface tension	5
3. The growth of stable drops	7
4. One-dimensional nozzle flow of a condensing vapour	8
5. An outline of the problem and its numerical solution	9
6. Data	10
7. Results	10
8. Discussion of results	11
8.1 Effects of varying surface tension	11
8.2 The effect of nozzle geometry on the collapse of the supersaturated state	11
8.3 The effect of reservoir conditions on the collapse of the supersaturated state	12
8.4 The mechanics of condensation	14
8.5 Comparison with experiment	14
8.6 Flow of a supersaturated vapour in a parallel duct	15
8.7 General discussion	17
8.8 Practical application and suggestions for further work	17
9. Conclusions	18
10. References	19
Appendix I	22
Appendix II	25
Tables	

## LIST OF SYMBOLS

### Greek

$\alpha$	condensed fraction defined as $\frac{m_d}{\rho} \frac{n_d}{d}$
$\gamma$	ratio of specific heats in vapour
$\delta$	constant factor in surface tension/radius relation
$\Phi$	chemical potential
$\rho$	density
$\sigma$	surface tension
$\Theta$	non-dimensional parameter in analysis of condensing flows, defined as $\frac{T_o^2}{290p_o^{\frac{1}{4}}} \cdot \frac{(K^2)^{0.025}}{(A_t)^{0.01}}$
$\tau$	transit time, defined as the time taken from the crossing of the saturation line to the appearance of 0.1% condensate (i. e. collapse of supersaturation)

### Nozzle parameters

$A_t$	nozzle throat area (in. <sup>2</sup> )	
$x$	streamwise ordinate, origin at throat (in.)	
$\theta$	nozzle expansion angle	
$K$	$= \sqrt{\pi} \cdot \tan \theta$	} Non dimensional nozzle parameters (see Fig. 2.)
$\xi$	$= \frac{K}{\sqrt{A_t}} \cdot x$	

### Subscripts

$o$	reservoir conditions
$\infty$	equilibrium value over a surface of infinite radius of curvature
$d$	droplet
$g$	vapour state
$l$	liquid state
$*$	nucleus of critical size.

### Superscripts

$D$	Diffusion speed
-----	-----------------

## LIST OF SYMBOLS

$a_f$	speed of sound at constant composition (frozen) defined by $a_f^2 = \gamma(1 - \alpha) RT$
A	flow area
C	constant in growth rate equations
$C_p$	specific heat at constant pressure
D	molecular diameter
h	enthalpy/unit mass
J	rate of formation of nuclei of critical size. (number/unit volume/ unit time)
k	Boltzmann's constant
$l_v$	latent heat of condensation
m	mass of molecule of vapour
$m_d$	mass of a liquid drop
M	Mach number defined as $M = q/a_f$
n	drop number density
N	total number rate of flow of drops
p	pressure (atm.)
q	flow speed
r	drop radius
R	gas constant for vapour
T	temperature ( $^{\circ}K$ )
W	rate of mass flow
x	streamwise nozzle co-ordinate.

### ACKNOWLEDGEMENTS

The author would like to take this opportunity of expressing his thanks to Professor G. M. Lilley and Mr. J. W. Cleaver for the many helpful suggestions which they made during the course of this investigation, and to Dr. S. Kirkby, and Mr. Ingham of the Department of Mathematics for their guidance in the use of the Pegasus Computer.

## 1. Introduction

When a perfect gas is expanded isentropically in a nozzle, the flow properties at any point can be determined knowing the reservoir conditions, the ratio of specific heats of the gas, and the nozzle geometry. Similarly, if a mixture of a vapour and its condensed phase is expanded in equilibrium, then knowing the Clausius-Clapyron vapour pressure relation for the gas in addition to the above, the flow properties can be calculated.

In hypersonic wind tunnel nozzles, where the flow is expanded to high Mach numbers (greater than 4.5), it can happen, for some reservoir conditions, that very low temperatures and pressures are reached and the line of isentropic expansion may cross the saturation line for the vapour. If this happens the expansion can continue in one of three ways.

- (a) An equilibrium saturated expansion
- (b) An isentropic expansion into the supersaturated regions.
- (c) A path somewhere between the two.

If (a) were followed, particles of condensed phase would begin to appear and this would limit the use of the flow for test purposes, while with (b) the composition and behaviour of the flow would remain unchanged. If (a) were followed, the rate of formation of the condensed vapour would have to be infinite at the commencement of condensation. However, since this rate will be finite, as shown below, we find in practice that a combination of all three paths is followed.

The fluid expands along the perfect gas isentrope (Fig.1) into the supersaturated region. At some point the supersaturated state breaks down and the expansion follows a path between the isentropic and saturated expansion curves. On intersection with the saturation line the expansion follows equilibrium saturation conditions down the remainder of the nozzle. The supersaturated state arises from the inability of the vapour to follow rapid changes in the flow conditions.

When condensation occurs in a gas it must take place either onto the walls of the confining vessel or onto nuclei suspended within the gas. In a nozzle flow problem the walls are effectively insulated from the main mass of fluid by the viscous boundary layer and, consequently, condensation must take place onto nuclei formed, or already existing, within the fluid.

In the condensation of a pure vapour, therefore, the condensation must take place on spontaneously formed nuclei. On the other hand, when a mixture of gases is considered, or traces of solid contaminant exist, condensation could take place on condensed droplets of a higher melting point gas, or on the solid contaminant (oil or dust particles), as well as on spontaneously formed nuclei.

As was mentioned above, the appearance of particles of condensed phase limits the use of the flow for test purposes. The normal method of avoiding this is either to raise the reservoir temperature, or to reduce the reservoir pressure to such an extent that the saturation line is not approached during the expansion. However, there are certain drawbacks involved in this. Raising the reservoir temperature involves the use of large and expensive heating installations, and if very high Mach numbers are desired the temperature in the reservoir might be above that at which dissociation occurs, if condensation in the working section is to be avoided. On

the other hand, lowering the reservoir pressure introduces the complication of low density flow in the working section and, in extreme cases, the risk of entering the slip flow region. It is therefore of interest to discover the extent of the supersaturated region and to investigate the possibility of testing within it.

Much theoretical and experimental work has been carried out on the condensation problem, originally of water vapour and the water content of humid air in supersonic wind tunnels, and more recently of the components of air in hypersonic nozzles. The physical treatment of droplets in a supersaturated vapour was first considered by Thompson<sup>(1)</sup> and Gibbs<sup>(2)</sup>. Of importance in the early investigations of the mechanism of nuclei formation was the work of Volmer<sup>(4)</sup>. This was greatly modified by later workers, particularly Becker & Döring<sup>(5)</sup>, Zeldovitch<sup>(6)</sup> and Frenkel<sup>(7)</sup>.

Oswatitsch<sup>(30)</sup> attempted a solution of the complete flow and achieved remarkable correlation with experiments on the condensation of water vapour by Yellot<sup>(29)</sup> and Binnie & Woods<sup>(28)</sup>. Using nuclei formation rates derived by Becker & Döring and knowing the rate of growth of the droplets, he was able to estimate the amount of condensed phase at any point in a nozzle. This, together with the normal continuity equations for a condensing fluid, enabled him to estimate the effect of condensation on the flow.

His excellent agreement with experiment was perhaps fortuitous, since in his calculations of the nuclei formation rate he neglected the variation of surface tension with drop size. Many workers, Tolman<sup>(10)</sup>, Kirkwood & Buff<sup>(11)</sup>, and particularly Reed<sup>(12)</sup> have since shown this to be significant on the small droplets concerned. Several attempts have been made to correct the condensation equations for this variation, first by Head<sup>(14)</sup>, and later by Stever & Rathbun<sup>(15)</sup> and Bogdonoff & Lees<sup>(9)</sup>. These various results differed widely however, Bogdonoff & Lees<sup>†</sup> producing results opposite to those of Stever & Rathbun.

The most systematic series of experiments on condensing flows have been performed at the Guggenheim Aeronautical Laboratory of the California Institute of Technology by Nagamatsu et al<sup>(16 - 20)</sup>. Important work has also been performed by Wegener & Smelt at N.O.L.<sup>(26)</sup>, Stever & Rathbun at M.I.T.<sup>(15)</sup> and McLellan & Williams at Langley Field<sup>(22)</sup>. In most experiments, condensation has been detected by a combination of light scattering and pressure plotting techniques. Wegener used the experimentally derived pressure distributions as the basis for an approximate theory, and by integrating the equations of motion was able to determine the temperature, velocity, and amount of condensed phase present at any point in the nozzle. Durbin<sup>(25)</sup>, on the other hand, using transmitted and scattered light data, was able to calculate drop sizes and particle densities in the condensed flow and from this, the amount of condensed phase present could be found.

Buhler & Nagamatsu<sup>(20)</sup> set up a theoretical analysis to back up the experimental work carried out at G.A.L.C.I.T. They considered the problem in three ways :-

- (i) An equilibrium saturated expansion
- (ii) A sudden collapse of the supersaturated state-----  
a condensation shock
- (iii) A study of the non-steady growth of drops in the  
supersaturated state and an integration of the  
drop growth to predict the nature of the collapse  
phenomenon.

They observed that the first two processes bracket the actual collapse and that the end state reached in each case was similar. Good correlation of the drop growth theory with experiment was also obtained. A thorough investigation of the effect of evaporation on passing a condensed flow through oblique and normal shocks was also made in the same report.

In this paper, a solution of the collapse of the supersaturated state was made following the method first used by Oswatitsch. The equations of motion were set up for a condensing vapour, and knowing the rate of growth of the condensed phase, a step by step numerical solution was carried out down the nozzle.

The condensation of a pure vapour (nitrogen) was first considered. The expression for nuclei formation rate suggested by Stever & Rathbun was used, together with the correction for the variation in surface tension by using Tolman's relation. Droplet growth rates were determined from simple kinetic theory. Numerical calculations were performed using a Ferranti "Pegasus" digital computer.

A systematic investigation was made of the effect of reservoir conditions and nozzle geometry on the collapse of the supersaturated state. It was found that an increase in reservoir temperature or nozzle expansion angle increased the supersaturation, whereas increasing reservoir pressure or nozzle length led to a decrease. The amount of supersaturation varied between  $8K^{\circ}$  and  $16K^{\circ}$ , and increments of 0.6 to 1.5 in Mach number were obtained for a range of reservoir conditions and nozzle geometries. In addition, an attempt was made to correlate certain experimental results obtained at Langley<sup>(22)</sup> and G. A. L. C. I. T. (16 - 20). Pressure distributions, drop sizes, and condensation particle densities were calculated, which agreed closely with the experimental values. This close agreement would seem to justify the application of the nuclei formation rate and surface tension correction employed.

An investigation was made into the effect of passing a vapour at various stages of supersaturation down a parallel duct. It was found that when the vapour was supersaturated at the entry to the parallel duct, a supercooling of about  $9.3K^{\circ}$  at a Mach number of 5.3 could be maintained for as much as four diameters down the duct without the flow departing significantly from a dry isentropic expansion.

## 2. The mechanics of condensation.

When a vapour is expanded to low temperatures and pressures in a nozzle, the working fluid is effectively insulated from the walls by the viscous boundary layer. Hence, condensation can only take place on spontaneously formed nuclei within the vapour and condensation on the walls does not occur.

## 2.1 Drop distribution

As a first step towards determining the rate of formation of nuclei, it is necessary to consider the conditions under which a small drop will be in equilibrium with its surrounding vapour. Early work on this problem was carried out by Thompson<sup>(1)</sup> and Von Helmholtz<sup>(3)</sup>, and later by Gibbs<sup>(2)</sup>. They arrived at a relation between the radius of the drop and the vapour pressure around it in terms of the volume of the liquid molecule, the saturation vapour pressure over a plane surface, and the temperature, which is

$$r_* = \frac{2v_1\sigma_\infty}{kT \log_e(p/p_\infty)} \quad (1)$$

where  $\sigma_\infty$  - surface tension over a surface of infinite radius of curvature

$v_1$  - liquid molecular volume given by the mass of the liquid molecule divided by the liquid density

$k$  - Boltzman constant

Equation (1) leads to the concept of a critical droplet size. If one molecule evaporates from the drop in equilibrium, evaporation will continue and, conversely, if one molecule condenses onto the surface the drop will continue to grow.

The nuclei are formed through fluctuations in density of the vapour near the critical state, and the distribution of droplets is given by the Gibbs' equation.

$$N = C \cdot \exp \left\{ - \Delta\bar{\phi}_g / kT \right\} \quad (2)$$

where  $N$  is the number of droplets of  $g$  molecules

$\Delta\bar{\phi}_g$  is the difference in thermodynamic potential between gaseous and liquid states.

$C$  is a constant term.

It may be shown<sup>(7), (43)</sup> that the energy of formation of drops has a maximum when the drops are of the critical size (given by equ. 1) and consequently the drop distribution has a minimum. Thus the Gibbs' equation gives a decreasing number of drops of increasing radius up to the critical radius, and then an increasing number of drops with further increase in radius. Frenkel<sup>(7)</sup> in a later analysis established the value of the constant  $C$  in equation (2).

## 2.2 Rate of formation of nuclei

In the expansions involved in a hypersonic nozzle, the change from stable and unsaturated, to unstable and supersaturated states occurs very rapidly. The processes involved may consequently be far from equilibrium, and the drop distributions obtained, assuming equilibrium conditions, will not be applicable. The problem is now one of finding how rapidly drops of a critical size form in the non-equilibrium conditions arising in rapid expansions of the flow.

The earliest significant work in this field was carried out by Volmer<sup>(4)</sup>. One of the main difficulties in finding the equilibrium supersaturated drop distribution is that after the critical droplet size has been reached, the number of drops increases with radius. This is clearly unacceptable. Volmer overcame this difficulty by setting the drop distribution equal to zero above some limiting radius. Further, since all nuclei must grow to the critical size and then continue to grow as stable droplets, he assumed the critical radius to be the limiting size. Volmer was then able to obtain a value for the nuclei formation rate using the above assumptions and simple kinetic theory. He found the rate of formation of droplets of critical size to be -

$$J = \frac{4\pi r_*^2 p^2}{(kT)^{3/2} \sqrt{2\pi m}} \exp \left\{ \frac{-4\pi \sigma_\infty r_*^2}{3kT} \right\} \quad (3)$$

where  $r_*$  is the critical radius given by equ (1) and  $m$  is the mass of a molecule

In his calculations Volmer made the significant error of only considering the growth to the critical size of smaller droplets. Later workers in the field, particularly Becker & Döring<sup>(5)</sup>, Zeldovitch<sup>(6)</sup> and Frenkel<sup>(7)</sup> noted this, and in their analyses allowed for the decay by evaporation of drops larger than the critical size.

Frenkel, using a non-equilibrium method first outlined by Becker & Döring and a solution suggested by Zeldovitch, arrived at an equation which gave the rate of formation of critical size droplets -

$$J = \frac{p^2 v_1}{(kT)^2} \left[ \frac{2 \sigma_\infty}{\pi m} \right]^{\frac{1}{2}} \exp \left\{ \frac{-4\pi \sigma_\infty r_*^2}{3kT} \right\} \quad (4)$$

where  $r_*$  is the critical radius given by equ (1).

If the exponential is expanded and  $r_*$  is substituted from equ. 1 it can be seen that it involves the cube of the surface tension, the square of the molecular volume of the liquid, and the vapour pressure. Since the expression is very sensitive to small changes in the exponential power (a change of 5% alters the answer by a factor of about 4, it is obvious that to ensure the accuracy of any numerical calculation these quantities must be defined with great care. This is not easy, since the molecular volume of the liquid depending on the density of the condensed drop and the vapour pressure, are both difficult to specify at low temperatures, whilst the surface tension, which varies with temperature, is also strongly dependent on the droplet radius in the critical region. In all the analyses described above, a constant value of the surface tension was assumed.

### 2.3 The effect of droplet size on surface tension

In regions of high nucleation rate the droplet is small, having a radius of only about 1.5 times the molecular diameter, and only contains between 12 and 15 molecules. Also, since the surface tension depends on the number of bonds

holding a molecule to the surface, it is clear that the addition of a molecule to a small droplet will have a greater effect than adding it to a larger drop. Since the last section showed that the value of surface tension must be known with some accuracy, it is obvious that the relationship between radius and surface tension must be determined.

Early work was performed on the problem by Gibbs<sup>(2)</sup> who came to the conclusion that the effect of curvature on surface tension would be small in typical cases until very small radii are considered (in the order of 10 - 20 Å) Tolman, in later work<sup>(10)</sup>, agreed with this, and using a quasi-thermodynamic argument he arrived at the following relation between surface tension and droplet radius -

$$\sigma = \frac{\sigma_{\infty}}{1 + \frac{2\delta}{r_*}} \quad \text{-----} \quad (5)$$

where  $\delta$  is some constant lying between 0.25 and 0.5 of the molecular diameter and  $\sigma_{\infty}$  is the surface tension over a plane surface.

This was later substantiated by Kirkwood and Buff<sup>(11)</sup> who arrived at a similar relation from a statistical mechanical argument. Mayer & Mayer<sup>(13)</sup> attempted a more thorough statistical mechanical approach to the problem but the method is too complex to be readily applied.

Bogdonoff & Lees<sup>(9)</sup> considered the problem from the aspect of crystal binding energies, and using work by Reed<sup>(12)</sup> and Taylor, Eyring & Sherman<sup>(31)</sup>, they obtained expressions for the energies of formation for small drops.

Stever & Rathbun<sup>(15)</sup> considered the geometry of surface molecule bonds and from this derived an expression connecting drop size and surface tension. -

$$\sigma = \frac{2}{3} \sigma_{\infty} \left[ 1 + \frac{(r_*^2 - r_* D)^{\frac{1}{2}}}{2r_* - D} - \frac{\sqrt{3}}{2} \cdot \frac{D}{2r_* - D} \right] \quad \text{-----} \quad (6)$$

where  $D$  is the molecular diameter.

The first attempt to correct the rate of nuclei formation for the variation of surface tension with radius was made by Head<sup>(14)</sup> who merely substituted Tolman's correction (equ. 5) into equation (4). On the other hand Stever & Rathbun recalculated the formation rate of critical nuclei assuming a variable surface tension and found -

$$J = v_1 \left[ \frac{p}{kT} \right]^2 \cdot \left[ \frac{2}{\pi m} \right]^{\frac{1}{2}} \left[ \sigma - r_* \frac{d\sigma}{dr_*} \right]^{\frac{1}{2}} \exp(B) \quad \text{-----} \quad (7)$$

where  $B = - \frac{8\pi}{kT} \left[ \int_0^r r_* \cdot \sigma \cdot dr_* - \frac{1}{3} r_*^2 \sigma \right]$

On substitution into (7) of the expression for surface tension given in equation (6) they found an increased nucleation rate, but Bogdonoff and Lees obtained a completely opposite result. The correction allowing for variations in the surface tension as found in this paper, is developed in full in appendix II.

### 3. The growth of stable drops

Once the condensation nuclei of critical size have formed, they continue to grow as stable drops of the condensed phase (liquid or solid). This steady growth dictates two conditions -

- (a) there must be a mass transfer to the drop due to collisions of molecules with the drop
- (b) there must be heat transfer away from the drop.

Condition (b) is necessary since, if the heat of condensation is not removed in some way, the temperature of the drop would rise until eventually it became unsaturated and growth would cease.

The heat transfer is achieved in two ways, depending on the size of the drop. When the drop is large compared with the molecular mean free path in the vapour and the vapour is assumed to be a continuum, the heat is removed by thermal conduction and the growth rate is given simply by -

$$\frac{dr}{dt} = \left\{ \frac{2k(T_1 - T)}{l_v \rho_1} \right\}^{\frac{1}{2}} \quad \text{_____} \quad (8)$$

where  $T$  is the droplet temperature,

$l_v$  the latent heat of condensation

$\rho_1$  the droplet density.

If, on the other hand, the drop is small compared with the mean free path in the vapour, then the heat is removed by molecular transport. Simple kinetic theory allows the rate of heat transfer to a surface and the number of molecules striking it per unit time to be easily calculated. Hence, on knowing the latent heat of condensation (or sublimation) and the mass of a molecule, the rate of growth may be determined(20). from -

$$\frac{dr}{dt} = \frac{1}{\rho_1} \frac{C_p p}{l_v} \left( \frac{k}{mT} \right)^{\frac{1}{2}} (T_1 - T) \quad \text{_____} \quad (9)$$

For nozzle flow problems this becomes the convective derivative  $\frac{Dr}{Dt} = \frac{\partial r}{\partial t} + q \frac{\partial r}{\partial x}$

and the gradient along the nozzle may be integrated to give drop sizes at any station, since, for the steady case,  $\frac{\partial r}{\partial t} = 0$ . The mass of the droplet is given by

$$m_d = \frac{4}{3} \pi r^3 \rho_1, \quad \text{where } r > r_*, \quad \text{therefore } \frac{dm_d}{dx} = 4 \pi r^2 \frac{dr}{dx} \cdot \rho_1 \quad \text{and}$$

$$\text{substituting from (9) above gives } \frac{dm_d}{dx} = 4 \pi r^2 \cdot \frac{C_p p}{q l_v} \cdot \left[ \frac{k}{mT} \right]^{\frac{1}{2}} \cdot (T_C - T) \quad \text{_____} \quad (10)$$

In a hypersonic nozzle drop sizes are, at all times, smaller than  $500\text{\AA}$ , so the above molecular transport growth rate applies.

#### 4. One dimensional nozzle flow of a condensing vapour

When a mixture of a gas and its condensed phase is expanding in equilibrium, the properties at any point in the flow may be calculated, if the Clausius-Clapyron vapour pressure curve is known in addition to the reservoir conditions and nozzle geometry. If, however, the expansion does not follow an equilibrium path and enters the supersaturated region, then additional information is required such as the amount of the condensed phase present, and the rate at which it is changing down the nozzle. The contribution to the mass flow rate of condensate past a station  $x$  in the nozzle, due to drops formed at some other station  $x'$  upstream, is -

$$W \cdot d\alpha = J(x') A(x') m_d(x', x) dx$$

where  $W$  is the total rate of mass flow,  $J(x')$  is the rate of formation of critical nuclei at  $x'$  where the flow cross section area is  $A(x')$ , and  $m_d(x', x)$  the mass of a drop formed at  $x'$  on arrival at  $x$ .

Consequently, the total of mass flow of liquid at  $x$  is given by -

$$W \cdot \alpha = \int_{x_0}^x J(x') A(x') m_d(x', x) dx'$$

where  $x_0$  is the point at which condensation commences as the expansion crosses the saturation line. Differentiation gives the rate of change of the amount of condensed phase present as -

$$\frac{d\alpha}{dx} = \frac{1}{W} \int_{x_0}^x J(x') A(x') \frac{\partial m_d}{\partial x}(x', x) dx' + J(x) A(x) m(x) - J(x_0) A(x_0) m(x_0)$$

It may be seen from equs. (1) and (2), Appendix 2, that  $J(x_0) = 0$  (since  $\log p/p_\infty = 0$  and  $r_* = \infty$ ) whilst at point  $x$  the drop, having only just formed is of negligible mass.

Consequently, the above may be written as -

$$\frac{d\alpha}{dx} = \frac{1}{W} \int_{x_0}^x J(x') A(x') \frac{\partial m_d}{\partial x}(x', x) dx' \quad \text{-----} \quad (11)$$

where  $\frac{dm_d}{dx}$  is the drop growth given by equ. (10).

The equations of conservation of mass, momentum, and energy may be derived for a mixed phase fluid and together with the condensation equation (equ. 11) can be solved simultaneously to determine the flow properties (Appendix 1).

In a condensed flow, the presence of particles of solid or liquid phase complicate the process which determines speed of sound and hence the Mach number. It can be shown that the speed of sound is the square root of  $\left(\frac{\partial p}{\partial \rho}\right)_S$  regardless of the

existence of particles of another phase, but the relation between pressure and density is strongly dependent on the interaction between the drops and the vapour. Several assumptions can be made as to the nature of this interaction<sup>(20)</sup>, each producing a different sound speed, but it is quite likely that none of them represents the interaction which takes place in practice.

In the analysis presented in this paper it has been assumed that the droplets are sufficiently small that they follow only velocity fluctuations, and that heat transfer does not take place between the drop and the vapour with the passage of a sound wave. This gives a sound speed (Appendix 1), which in fact is equivalent to the frozen sound speed

$$a_f = \sqrt{(1 - \alpha) \gamma RT.}$$

where  $\alpha$  is amount of flow condensed,  $\gamma$  the ratio of specific heats, and R the gas constant for the vapour.

#### 5. An outline of the problem and its numerical solution.

It was desired to obtain a solution of the problem of condensing flows, along the lines suggested by Oswatitsch<sup>(30)</sup>, to obtain some idea of the effect of reservoir conditions and nozzle geometry on the supersaturation to be expected, to determine the effect of passing a vapour with different degrees of supersaturation into a parallel duct, and to attempt to reproduce theoretically some of the mass of experimental results which exist (15 - 20).

The expansion considered is broken into three parts -

- (i) A dry isentropic expansion
- (ii) A process following some path in the supersaturated region.
- (iii) An equilibrium saturated expansion.

In the unsaturated region, solution of the flow equations is quite straightforward. As soon as the expansion crosses the saturation line and enters the supersaturated region (Fig.1) however, condensation nuclei begin to form. At first the critical nuclei are large since  $p \approx p_\infty$ , and consequently the rate of formation is small. As the supersaturation increases, the radius is reduced (equ.1), and the rate of formation of nuclei increases.

Since the amount of condensed phase depends on the rate of formation of drops and their subsequent growth, it is obvious that the flow will expand some way into the supersaturated region before a significant amount condenses. When this occurs, the flow will leave the isentropic expansion it has been following, the temperature will rise due to the condensation heat release, and the flow will enter the region approaching the saturation line. (Fig.1). When saturation conditions are again reached, the flow follows a saturated expansion curve down the remainder of the nozzle.

The actual expansion met in practice is only slightly different from the idealised picture given here. The expansion rejoins the saturation line with a slight fairing of the sharp corner shown in Fig.1, and thereafter follows a saturation line at a slightly lower temperature than that for a plane surface because of the loss in energy involved in the formation of the droplets. Experiments show these effects to be small.

The solution is commenced in the unsaturated region. At some point in this region close to the saturation line, knowing the flow properties and nozzle geometry, the conservation equations are solved to give the variation of pressure, density, and velocity along the nozzle. An iterative process<sup>(34)</sup> is used whereby the flow properties and their variation are calculated at an adjacent point and then, using the mean variation of the flow properties at the first and second points, the properties at the second point are recalculated. When the difference between two calculated values at the second point is within a specified accuracy, the calculation moves on and, using the second point as a base, the flow properties at the third point are calculated and so on. This step by step solution is carried out down the nozzle until the saturation line is crossed for the first time.

In the supersaturated region, the critical nucleus size and the corresponding rate of formation of critical sized nuclei are calculated at each point. The radius of stable drops is determined by integration using Young's Quadrature<sup>(35)</sup>, and from this the rate of growth of the droplets is found. This growth rate together with the rate of formation of nuclei and nozzle cross section area enables another integration to be performed, commencing at the saturation point and extending to the point at which the flow is required, and so the variation in the amount of condensed phase is determined. Using this additional information, the flow equations are again solved as described above. This process continues down the nozzle until the saturation line is again intersected.

The equilibrium saturated expansion is found simply from a simultaneous solution of the three continuity equations and the Clausius-Clapyron vapour pressure relation.

Since the iterative solution is rather tedious and involved if great accuracy is desired, it was decided to programme the equations for solution on a Ferranti "Pegasus" digital computer. This was done using the "Autocode" system, and it was found convenient to non-dimensionalise the equations in order to facilitate the checking and input of data.

## 6. Data

The main drawback in calculations of the low temperature behaviour of gases is the lack of precise knowledge of their physical properties. Throughout the calculations, the N.B.S. Circular 564, republished by Pergamon Press<sup>(36)</sup>, was used for the thermodynamic properties of the gaseous state. The expression used for the vapour pressure in the solid state also came from this source. Surface tension in the solid state was taken from work by Aoyama & Kanda<sup>(38)</sup>. No data were available on the density of nitrogen in the solid state and this had to be extrapolated below 68°K from liquid nitrogen densities given in the International Critical Tables<sup>(37)</sup>. Heats of condensation and sublimation were also taken from this reference.

## 7. Results

Computations were made over a wide range of reservoir conditions and nozzle geometries for nitrogen. The results obtained from the computer for the pressure, temperature, and condensate distribution in the nozzles are shown in Figs. 5 to 19. In addition, temperature gradients and transit times were obtained for all nozzle geometries. In all cases the supercooling, condensation Mach number, and nuclei

formation rate at collapse were read from the computer print out. All results are summarised in Table I.

Several calculations were made on the effect of passing vapour in varying degrees of supersaturation down a parallel duct and the results are presented in Figs. 34 - 35, and Table 2.

Since one of the main difficulties in experiments is the determination of the exact point of deviation from the isentrope, it was decided to assume that collapse of the supersaturated state occurred when 0.1% of the flow had condensed. This seemed to give a fair indication, since on most plots the appearance of 0.1% condensate and departure from the isentrope were almost simultaneous.

From the mass of results obtained a chart for the analysis of condensed nitrogen flow in the supersaturated region has been prepared and is presented in Fig. 20.

## 8. Discussion of Results

### 8.1 Effects of varying surface tension

In the derivation of the nuclei formation rate it was seen that the variation of surface tension with droplet size was an important factor in the calculation. The correction suggested by Tolman<sup>(10)</sup> was used with  $\delta = 0.5D$  (see Equ. 5), as suggested by Stever. An attempt was next made to provide theoretical data for the experimental case (run 9 - 5, Ref. 16) but the agreement was extremely poor. This prompted an investigation into the effect of the varying surface tension on the nuclei formation rate and condensation.

Calculations were made using different values of  $\delta$  and the results are plotted in Fig 4. It can be seen that altering the value of  $\delta$  from  $0.5D$  to  $0.25D$  has little effect on the total value of the nuclei formation rate. The area under the curve is changed considerably, however, and the maximum moved some way down the nozzle. Both these factors influence the amount of condensed phase present and the eventual collapse of the supersaturated state. From Fig. 4 it can also be seen that with a constant value of surface tension ( $\delta = 0$ ) there is little likelihood of enough condensation occurring to influence the supersaturated state.

In order accurately to fix  $\delta$ , it was decided to find a value which gave good agreement with one set of experimental results. If this value, used in subsequent calculations, gave good agreement with completely different experiments, then the original assumption would be taken as justified. This was done, and the value of  $\delta$  which gave best agreement with the experimental curve was found to be  $1.15\text{\AA}$  or 0.36 times the molecular diameter.

### 8.2 Effect of nozzle geometry on the collapse of the supersaturated state

The effect of changes in nozzle expansion angle and throat area on the collapse of the supersaturated state, pressure distribution, and amount of condensed phase present are shown in Figs. 14 to 22. Increasing the throat size and reducing the expansion angle decreased the supersaturation obtained. Since altering the expansion angle or the throat size for a given nozzle area ratio changes the length of the nozzle, it can be seen from the above that factors dependent on nozzle size,

temperature gradient and time between saturation and condensation are functions of the degree of supercooling obtained. This is shown in Figs. 23 & 24. At constant reservoir conditions ( $p_o = 8.3 \text{ atm.}$   $T_o = 290^\circ\text{K}$ ) an increase in transit time (from saturation to condensation) means a reduction in the supercooling expected.

The appearance of condensation is determined by nucleation. Consequently, the longer the period available for nucleation, the nearer the flow is to equilibrium and the less intense the supersaturation attained. Kantrowitz<sup>(8)</sup> shows that the transit time should be proportional to the fourth power of the supercooling and this is plotted on Fig. 23. The theory developed by Kantrowitz was for the supersaturation of water vapour. This explains the deviation at the lower values of supercooling, because the assumptions Kantrowitz makes about relative times involved in the process are not strictly valid in this region, where the degree of supercooling is much smaller.

Since the supercooling of the vapour is a function of its inability to follow rapid temperature changes down the nozzle, some correlation between supercooling and temperature gradient is to be expected. This is shown in Fig. 24. An increase in temperature gradient gives an increase in the degree of supercooling.

After completing the collapse stage of condensation and attaining equilibrium, the amount of flow condensed is the same, irrespective of the geometry of the nozzle in which it was obtained. From this it can be deduced that the total number of droplets formed must be the same in each case. It can then be further deduced, since the temperature gradient and transit time are functions of supercooling, that the rate of formation of nuclei is also a function of supercooling. This is brought out in Fig. 25. A high degree of supercooling demands a low transit time and a large temperature gradient, and consequently a high rate of formation of nuclei.

One case computed deserves special comment. That is the point with  $K^2 = 1.0$  and  $A_t = 0.01 \text{ in}^2$ . Fig. 14 shows that in this case departure from the isentropic curve is very gradual and not marked by a sudden increase in temperature as in other cases. It is thought that this is due to a difference in the mechanism of condensation. In this case the expansion is very rapid (the semi angle of the nozzle being about  $30^\circ$ ) and nucleation is never properly established. Consequently, the bulk of the condensation is due to the slow growth of a few droplets formed some way up the nozzle (rather than by condensation on a large number of small drops formed later.)

### 8.3 The effect of reservoir conditions on the collapse of the supersaturated state

The effect of varying stagnation conditions on the collapse of the supersaturated state and the distribution of pressure, temperature, and the amount of condensate present is shown in figures 5 - 12. The path followed by the collapse is similar to that caused by the variation in the nozzle geometry. It can be seen that increasing the reservoir pressure from 8.3 to 70 atm. at  $290^\circ\text{K}$  causes a reduction in the degree of supersaturation from  $11.85^\circ\text{K}$  to  $7.3^\circ\text{K}$ . A further increase in the reservoir pressure to 100 atm. shows an increase to  $8.8^\circ\text{K}$ . This trend is repeated at higher reservoir temperatures and at  $450^\circ\text{K}$  the supercooling ranges from a maximum of  $15.1^\circ\text{K}$  at 8.3 atm. to a minimum of  $10.9^\circ\text{K}$  at 70 atm.

The variation of reservoir temperature at constant pressure produces an increase in supercooling with increasing temperature. With a reservoir pressure of 70 atm. a range of supercooling is obtained from 7.3°K with  $T_o = 290^{\circ}\text{K}$  to 10.9°K at  $T_o = 450^{\circ}\text{K}$ . At lower reservoir pressures, however, raising the reservoir temperature seems to have less effect beyond  $T_o = 350^{\circ}\text{K}$ , and the curve gradually flattens out to give a maximum of 15.1°K supercooling at  $T_o = 450^{\circ}\text{K}$  and  $p_o = 8.3$  atm. The degrees of supersaturation obtained for the various conditions are summarised in Fig. 21.

The reason for this variation in the degree of supersaturation is quite easily seen on consideration of Fig. 36. together with the equations for critical drop size and rate of nucleation (see Equ. (1) and (2) in Appendix 2). Figure 36 is a plot on the temperature/pressure plane of the equilibrium saturation line and three isentropic expansions. It can be seen that the slope of the saturation line decreases with increasing temperature, and the ratio between vapour and saturation pressure, at a given supercooling, decreases with increasing reservoir pressure or decreasing reservoir temperature.

The collapse of the supersaturated state depends primarily on nucleation, and the rate of formation of nuclei is governed by the critical nucleus state, the surface tension, and the temperature. At low temperatures, because the reduced temperature and increased surface tension will be more significant than the reduced molecular volume and increased pressure ratio, the critical radius for a given degree of supersaturation will be larger than at a higher temperature. Consequently, the rate of formation of nuclei will be retarded, since it depends not only on droplet size but also on the surface tension and the inverse of the temperature in the exponential power (Equ. (1) Appendix 2). Thus the supercooling will be increased.

As the temperature is increased, the pressure ratio and temperature terms become of equal significance and, as shown in Fig. 21, the supersaturation curve reaches a minimum at a reservoir pressure of about 70 atm. For higher reservoir pressures it can be seen, from Fig. 36, that the pressure ratio becomes further reduced for a given supercooling. Since the pressure ratio appears in the denominator of the critical radius expression (Equ. (2) Appendix 2), and the temperature terms are now less significant, the radius of the nucleus increases and the rate of formation of nuclei is decreased. Supercooling is consequently greater.

This explains the increase in supercooling with increased reservoir temperature and the decrease, with increased reservoir pressure up to 70 atm, because changing the reservoir conditions only moves the point of intersection of the isentropic expansion with the saturation line.

No attempt was made to correlate the transit times or temperature gradient for the cases where the reservoir conditions were varied. Curves similar to Figs. 23 and 24 could be determined, however, if the nozzle geometry was varied at each stagnation condition. Rates of formation of nuclei are plotted in Fig. 26.

#### 8.4 Mechanics of Condensation

Although the rate of formation of nuclei was obtained for all the cases computed, for convenience only one case (see Fig. 3) has been presented graphically. The peak value occurs almost simultaneously with the collapse of the supersaturated state. As soon as the saturation line is crossed, nucleation commences but does not become significant until appreciable degrees of supersaturation are reached. (In Fig. 3 this occurs about  $\xi = 5.4$ ). Beyond this point the temperature continues to drop and supersaturation increases. Consequently, the radius of the critical droplet is reduced (Equ. 2 Appendix 2) and the rate of formation of nuclei is increased until a significant amount of condensate has formed. The rate of temperature drop is reduced until at the collapse point a minimum temperature is reached (Fig. 1). As the expansion continues the temperature increases, the supersaturation is reduced, and consequently the size of the critical drop increases. This, coupled with the rise in temperature, reduces the rate of formation of nuclei till it again becomes insignificant.

The total number of drops passing any plane in the nozzle is simply the integral of the product of nucleation rate and flow cross-section area at a point between the commencement of condensation and the point considered. It can be seen from Fig. 3 that the total number of drops present becomes sensibly constant once the nuclei formation rate is no longer significant. Once the total number of droplets existing is known the drop densities can be calculated at any section by dividing the total by the product of the cross-section and the stream velocity at that point.

Since the rate of increase of condensate depends on the integral of the nucleation rate and stream area (Equ. 11), it is to be expected that once the formation of nuclei becomes insignificant (less than  $0.5 \times 10^{17}$  in Fig. 3) the amount of condensed phase present will grow linearly beyond  $\xi = 6.8$  until it meets the saturation line.

The assumption made by several workers in the field, particularly Hansen & Nothwang<sup>(21)</sup>, that a constant value of nuclei formation rate could be used as a "threshold" for condensation, is shown to be erroneous. Besides being sensitive to changes in reservoir temperature, acknowledged by Hansen & Nothwang, it is also very sensitive to changes in nozzle geometry. This is shown in Fig. 25 and is discussed in section 7.2 above. The nucleation rates for all the cases computed are presented in Fig. 26 against the degree of supercooling, with curves drawn through the values at constant reservoir conditions.

#### 8.5 Flow of a supersaturated vapour in a parallel duct.

In the three previous sections it has been shown that the collapse of the supersaturated state is due, in most normal cases, to the nucleation and growth of large numbers of nuclei close to some point determined by reservoir conditions and nozzle geometry. It must be expected, therefore, that if a gas is expanded to some point just below the collapse and then passed down a parallel duct, the supersaturation should be sustained. To verify this the calculation was modified so that at any specified station in the nozzle the expansion could be stopped and the flow passed down a constant area duct.

For a reservoir pressure and temperature of 8.3 atm. and 290 K and a throat area and expansion factor of  $0.01 \text{ in}^2$  and 0.03886 respectively the flow was expanded to varying degrees of supersaturation. The expansion was then halted and the flow passed down the constant area duct for 4 diameters. Results are summarised in Table 2 and Figs. 34 and 35.

It is found that if the expansion is stopped before nucleation is properly established, the supersaturation is sustained. If however, sufficient nuclei exist at the end of the nozzle then condensation onto them is sufficient to cause reduction in the supercooling. This effect increases until, if the flow enters the parallel duct after the supersaturation has begun to collapse, condensation on existing drops is enough to return the flow to the saturation line (Fig. 34).

Figure 35 shows this effect on the pressure distribution. In the ideal case, where supersaturation is sustained, the pressure remains constant. When condensation occurs, however, the pressure rises due to the condensation heat release and in the extreme case, rises until it reaches the equilibrium saturated value and thereafter remains constant.

For the conditions used here, an area ratio of about 31 would be ideal giving a supercooling of  $9.3\text{K}^{\circ}$  at a Mach No. of 5.3 even after 4 diameters of a parallel duct. This corresponds to a number density of droplets of  $5 \times 10^{10}/\text{cc}$  of mean radius  $130\text{\AA}$  approximately at the end of the expansion.

#### 8.6 Agreement with Experiment

After having established accurately the value of the factor  $\delta$  using one experimental result, an attempt was made to reproduce theoretical results corresponding to further experiments performed at G.A.L.C.I.T. and Langley. The particular experiments were.

- (i) run 13-2 in ref. 16., pressure and condensate distributions and pressure-temperature variation.
- (ii) ref. 19., experimental variation of supersaturation and condensation Mach number with varying reservoir conditions.
- (iii) ref. 22., pressure distribution, drop sizes, and particle density.

#### (i) Comparison with ref. 16.

Agreement with the measured pressure distribution is extremely good and within the experimental scatter (Fig. 27). The agreement with the values of condensed phase present appears to be poor (Fig. 28.), but since the amounts given in ref. 16. are computed, and have a quoted reliability of  $\pm 20\%$ , the difference is not as severe as it appears. Because of the excellent tie up between theoretical and experimental pressure distributions, the disparity between the two in the pressure/temperature plane (Fig. 29) is surprising. It cannot be explained by simple scatter, since a limit of  $\pm 2.5^{\circ}\text{K}$  is quoted, and must be due to some more fundamental cause. The good agreement with the experimental pressure distribution is thought to be sufficient to justify the present theory in this case.

(ii) Comparison with ref. 19

Experimental data on condensation Mach number (i.e. Mach number at collapse) were available over a range of reservoir pressures from 4 - 20 atm. and temperatures up to 360°K (Fig. 30). Correlation is good at the lower reservoir temperature over the whole pressure range. The theoretical curve lies within the quoted scatter band ( $\pm 0.1$  Mach no. at 8.3 atm., 290°K). Agreement is not as good at the higher temperature, but if the scatter is assumed to be proportional to reservoir conditions, the theoretical line is still within the scatter band. The trend of the theoretical curve towards lower condensation Mach numbers at higher reservoir pressures is quite well substantiated at the 290°K reservoir temperature. It appears from the reference that the Mach number given is calculated from measured static pressures and consequently comparison with the theoretical Mach number is justified.

Figure 31 compares the theoretical and experimental variation of supersaturation with reservoir conditions. It can be seen that the trends, with increase in both temperature and pressure, are completely opposed. This difference is very surprising in view of the excellent agreement, both with regard to values and the trend, obtained with condensation Mach number. No explanation can be offered for this difference since it contradicts the theory put forward in section 8.3 of this discussion. Nagamatsu and Arthur quote results from a report<sup>(41)</sup> which they claim follow the trend of their experiments. Further investigation of this source, however, showed good agreement with the present theory at reservoir temperatures up to 500°K and pressures up to 35 atmospheres (Fig. 31). Beyond this, if an extrapolation is made based on Fig. 21, there is good agreement at even higher temperatures and pressures.

(iii) Comparison with ref. 22

Results from ref. 22 are plotted on Figs. 32 and 33 with the theoretical values inserted for comparison. Agreement with the pressure distribution is reasonable, but it is unfortunate that over the region of particular interest the pressure was not measured. It is reasonable to expect some supersaturation, since the level of impurities is low (less than one part per million of water vapour and approximately 0.01% of carbon dioxide).

The experimental and theoretical distributions were matched using a pressure plot obtained during a heated run where no condensation occurred. Better agreement is reached, however, with the drop sizes and particle densities (Fig. 33). At the 3.3" station the theoretical value lies within the experimental scatter. At the 2.4" station the calculated point lies below the experimental, but this is to be expected if slightly less supersaturation is assumed because of the presence of some impurity. A particle density of  $33 \times 10^8$  per cc. was calculated at the 3.1" station. This would be equivalent to a test section particle density of approximately  $10 \times 10^8$  per cc., smaller, by a factor of 3 x, but of the same order of magnitude as the experimental result ( $32 \times 10^8$  per cc.) Because the nature of the assumptions made in the scattered and transmitted light experiments, (that all particles were the same size, of spherical shape, and constant refractive index of 1.2) order of magnitude accuracy is all that can be expected and the above agreement is thought to be satisfactory.

### 8.7 General Discussion

As would be expected when the lines of collapse in the temperature/pressure plane were considered, it was found that each case followed a similar line. This led to the expression of all four variables ( $p_o$ ,  $T_o$ ,  $A_t$ , &  $K^2$ ) in one quantity

$\Theta$  From the mass of results obtained it was then possible to plot lines of constant  $\Theta$  (i.e. lines of collapse) on the pressure/temperature plane. This is done in Figure 20. In addition, lines of constant area ratio, Mach number, and amount of flow condensed are shown. Figure 20 can now be used as a chart for the analysis of condensed flows in the supersaturated region. For the analysis of a particular flow,

- (i) On Fig. 20 draw the equilibrium saturated line for the reservoir conditions to be used.
- (ii) From the nozzle geometry and reservoir conditions calculate  $\Theta$ . This gives the line of collapse.
- (iii) Follow the expansion down the isentrope.

If the desired expansion is completed before the saturation line is crossed the flow will be unsaturated. If the expansion crosses the saturation line, enters the supersaturated region, but is completed before the  $\Theta$  value is reached, the analysis can go no further since the values calculated are for continually expanding flows. If, however, the  $\Theta$  value for the flow is reached, the expansion will continue down the collapse line and the saturation line until the desired area ratio is attained. Pressure, temperature, Mach number and amount of condensate present can be determined from the diagram.

In a calculation of this kind, where computation is carried out by a high speed digital computer, the only factor influencing the accuracy of the results is the precision with which the data are specified. At all times in this work, assuming the data to be reliable, the precision of the presented results is limited by the accuracy of hand plotting.

### 8.8 Practical Application and suggestions for further work

It is doubtful whether the low degrees of supercooling predicted in this paper would be of any real use to the experimenter. The results have shown, however, that it should be possible to reduce considerably the heating required to prevent the appearance of condensed phase in high Mach number wind tunnels operating with condensable gases.

The results obtained in this paper are for a 100% pure gas (nitrogen), very seldom obtained in practice but attainable with careful filtering and drying. In order to represent more accurately a real fluid, the problem of condensation of mixtures of gases and the condensation of gases with traces of solid, liquid, or gaseous contamination should be investigated.

9. Conclusions

The conclusions that may be drawn from the computations performed may be summarised as follows.

- (a) In all but the most rapid expansions, nucleation is the mechanism which triggers off the collapse of the supersaturated state.
- (b) For any given set of reservoir conditions an increase in temperature gradient will give greater supercooling. Thus in a larger nozzle, or one with a smaller expansion angle, less supersaturation may be expected.
- (c) With increase in the reservoir temperature, or a reduction in the reservoir pressure, the supercooling is increased.
- (d) Some limit would appear to exist in the increase in supercooling with increase in reservoir temperature at  $T_0 = 450^\circ\text{K}$ .
- (e) Because of the relative shapes of the isentropic and saturated expansion curves, a minimum exists in the reduction of supercooling with increased reservoir pressures at 70 atm. At higher pressures the supercooling increases.
- (f) It is possible, if conditions are properly chosen, to pass an expanded supersaturated vapour along a constant area duct for 4 diameters and still maintain a high degree of supercooling.

10. References

1. Thomson, Sir. W., Lord Kelvin Proc. Roy. Soc. Edinburgh, Vol.11, 1870, pp. 63-68.
2. Gibbs, J.W. Collected works. Longmanns, Green & Co. Ltd., 1931.
3. Von Helmholtz, R. Untersuchungen uber Dampfe und Nebel, besonders uber solche von Losungen. Ann. Physik., Bd. 27, Heft, 4, pp.508-543, 1886.
4. Volmer, M. Kinetic der Phasenbildung, Dresden, Steinkopff, 1939.
5. Becker, R. and Doring, W. The kinetic treatment of nuclei formation in supersaturated vapours. Ann. Physik., Vol.24, 1935, p.719 and NACA TM. 1374
6. Zeldovitch, YB. J. Exptl. Theor. Phys., U.S.S.R., Vol.12 1942, pp. 525-538.
7. Frenkel, J. Kinetic theory of liquids. Oxford, Clarendon Press, 1946.
8. Kantrowitz, A. Nucleation in very rapid vapour expansions. J.Chem. Phys., Vol. 19, 1951, pp. 1097-1100.
9. Bogdonoff, S.M. and Lees, L. Study of the condensation of the components of air in supersonic wind tunnels. Part 1. Absence of condensation and tentative explanation. U.S. Nav. Ord. Lab., Symposium on Aerothermodynamics, June 1949. (N.O.L.R. 1134.)
10. Tolman, R.C. The effect of droplet size on surface tension, J.Chem. Phys., Vol. 17, 1949, pp. 338 -343.
11. Kirkwood, J.G. and Buff, F.P. The statistical mechanical theory of surface tension. J.Chem. Phys., Vol. 17, 1949, pp. 333-337.
12. Reed, S.G. On the early stages of condensation of rare gas type molecules. J.Chem. Phys., Vol. 20, 1952, pp. 208-211.
13. Mayer, J.E. and Mayer, M.G. Statistical mechanics. Wiley, 1940.
14. Head, R.M. Investigation of spontaneous condensation phenomena. Ph.D.Thesis, Cal.Tech., 1949.
15. Stever, H.G. and Rathbun, K.D. Theoretical and experimental investigation of condensation of air in hypersonic wind tunnels. NACA TN 2559, 1951.
16. H. T. Nagamatsu & W.W. Willmarth Condensation of Nitrogen in a hypersonic nozzle. G. A. L. C. I. T., W/T. Memo 6, Jan. 1952.

17. H. T. Nagamatsu & P. D. Arther "Effects of impurities on the supersaturation of nitrogen in a hypersonic nozzle". G. A. L. C. I. T., W/T Memo 7, March 1952.
18. H. T. Nagamatsu & J. Grey "The effects of air condensation on properties of flow and their measurement in hypersonic wind tunnels". G. A. L. C. I. T., W/T. Memo 8, June. 1952.
19. H. T. Nagamatsu & P. D. Arther "Experimental supersaturation of gases in hypersonic wind tunnels". G. A. L. C. I. T., W/T. Memo 10. July 1952.
20. H. T. Nagamatsu & R. D. Buhler "Condensation of air components in hypersonic wind tunnels - theoretical calculations and comparison with experiment". G. A. L. C. I. T., W/T. Memo 13, December 1952.
21. C. F. Hansen & G. J. Nothwang. "Condensation of Air in supersonic wind tunnels and its effect on flow about models" N. A. C. A. TN. 2690, 1952.
22. C. H. McLellan & T. W. Williams "Liquifaction of air in the Langley 11 inch hypersonic tunnel". N. A. C. A. TN. 3302 1954.
23. P. P. Wegener "Summary of recent experimental investigations in the N. O. L. Hyperballistics wind tunnel". J. Aero. Sci., Vol. 18, 1951. pp. 665-670.
24. W. T. Strike & W. N. MacDermott "The effects of liquifaction of air on the pressure distribution and forces on a cone-cylinder body at  $M=5.0$ ". A. E. D. C. -T. N. - 57 - 14. June 1957.
25. E. J. Durbin. "Optical methods involving light scattering for measuring size and concentration of condensation particles in supercooled Hypersonic flow". N. A. C. A. TN. 2441, 1951.
26. Wegener, P. P. and Smelt, R. Summary of Naval Ordnance Laboratory research on liquifaction phenomena in hypersonic wind tunnels. U.S. Nav. Ord. Lab. Memo. 10772, 1950.
27. Wilde, K. A. Condensation in nozzles. J. Appl. Phys. Vol. 30, 1959, p. 577.
28. Binnie, A. M. and Woods, M. W. The pressure distribution in a convergent-divergent steam nozzle. Procs. Inst. of Mech. Engrs., Vol. 138, 1938, p. 229.
29. Yellot, J. I. Supersaturated steam. Engineering, Vol. 137, 1934. p. 303



11. Appendix 1

Derivation of the Equations

Assumptions

- (i) Liquid drops are at all times sufficiently small (less than  $500\text{\AA}$  diameter)
- (ii) Density of liquid  $\gg$  density of vapour.
- (iii) Liquid drops may be treated as molecules of a 'heavy gas'.
- (iv) The flow is inviscid, non-heat conducting and diffusion effects are ignored.
- (v) The vapour is a thermally perfect gas.

Thus, for a vapour  $N_2$ , say, condensing into drops,  $D$ , the equation for the reaction is



where  $n$  is a large number.

The law of mass action gives

$$\frac{p_1^n}{p_2} = K(T) \quad \text{where } p_1 \text{ and } p_2 \text{ are the}$$

partial pressures of the vapour and liquid respectively, and approximately  $p = p_1$

The equilibrium constant  $K(T)$  is given by the Clausius-Clapyron relation.

$$\frac{d}{dT} (\log_e p) = \frac{d}{dT} (\log_e K) = \frac{lv}{RT^2}$$

where  $lv$  is the heat of vaporization per unit mass.

If the suffices  $1$ , and  $2$ , represent the vapour and droplet respectively then the one dimensional equation of continuity for the droplets is

$$\frac{d}{dx} \left\{ \rho \alpha A (q_2 + q_2^D) \right\} = A \int_{x_0}^x K_2(x', x) dx'$$

where  $K_2$  is the mass rate of production of droplets,  $x'$  is the position of drop formation, and  $x_0$  the point at which the process crosses the saturation line.  $q$  is the mass average velocity and  $q^D$  the diffusion velocity. Due to the assumptions made above, we can put  $q_1 = q_2$  and  $q_2^D = 0$  so that

$$\frac{d}{dx} \left\{ \rho \alpha A q \right\} = \rho A q \frac{d\alpha}{dx} = A \int_{x_0}^x K_2(x', x) dx'$$

since the equation of continuity is  $\rho A q = \text{constant}$ .

A similar expression can be found for the vapour but on noting that

$$K_2(x, x') = -K_1(x, x')$$

and

$$\rho \alpha q_2^D = - (1 - \alpha) \rho q_1^D,$$

we see that this equation reduces identically to that obtained for the droplets.

The one-dimensional equation of motion for the flow of the inviscid mixture is

$$\rho q \frac{dq}{dx} + \frac{dp}{dx} = 0$$

The one-dimensional equation of energy becomes

$$\rho q A \frac{d}{dx} (h + q^2/2) = \frac{d}{dx} \left\{ A \rho \alpha q_2^D (h_1 - h_2) \right\}$$

where  $h_1 - h_2 = l_v$ , the heat of vaporization. But  $h = h_1 + \alpha(h_2 - h_1) = h_1 - \alpha l_v$  and since  $q_2^D = 0$  we find  $\rho q \frac{d}{dx} (h_1 + q^2/2 - \alpha l_v) = 0$ . or  $h_1 + q^2/2 - \alpha l_v = \text{constant}$ .

We also find that for the range of temperatures considered the specific heat at constant pressure for the vapour is nearly constant, or

$$h_1 \approx C_{p1} T$$

and from the equation of state

$$p \approx p_1 = \rho (1 - \alpha) R_1 T$$

where  $R_1$  is the gas constant for the vapour.

The speed of the head of the wave propagating from a small disturbance in the flow is equal to the speed of sound,  $a_f$ , evaluated at constant composition, and it may be shown that

$$a_f^2 = \gamma (1 - \alpha) R_1 T \frac{\left\{ 1 - \frac{\alpha l_v}{R_1 T} \cdot \frac{\gamma - 1}{\gamma} \right\}}{\left\{ 1 - (\gamma - 1) \frac{\alpha l_v}{R_1 T} \right\}}$$

$$\approx (1 - \alpha) \gamma R_1 T = \frac{\gamma p}{\rho} \quad \text{when} \quad \frac{\alpha l_v}{R_1 T} \ll 1.$$

is the ratio of specific heats for the vapour.

The Mach number may now be defined as

$$M = q/a_f$$

then 
$$\frac{1}{p} \frac{dp}{dx} = - \frac{\gamma M^2}{q} \cdot \frac{dq}{dx} = \gamma M^2 S, \text{ say,}$$

with 
$$\frac{1}{\rho} \frac{d\rho}{dx} = S - \frac{1}{A} \cdot \frac{dA}{dx}$$

and 
$$-\frac{1}{q} \cdot \frac{dq}{dx} = S = \frac{\frac{1}{A} \cdot \frac{dA}{dx} + \left\{ \frac{1}{1-\alpha} - \frac{lv}{C_p \cdot T} \right\} \frac{d\alpha}{dx}}{\left\{ 1 - (1-\alpha+\alpha\gamma)M^2 \right\}}$$

-----

12. Appendix 2.

The variation of the critical radius and nucleation rate with variable surface tension.

The expression for rate of formation of critical sized nuclei assuming a surface tension varying with radius was found by Stever and Rathbun to be

$$J. = v_1 \left[ \frac{p}{kT} \right]^2 \left[ \frac{2}{\pi m} \right]^{\frac{1}{2}} \left[ \sigma - r_* \frac{d\sigma}{dr_*} \right]^{\frac{1}{2}} \exp. B$$

where

$$B. = - \frac{8\pi}{kT} \left[ \int_0^{r_*} r_* \sigma. dr_* - \frac{1}{3} r_*^2 \sigma \right]$$

$$\sigma = f(r)$$

and r is given by 
$$r_* = \frac{2v_1 \sigma}{kT \log_e (p/p_\infty)}$$

In this paper, Tolman's<sup>(10)</sup> expression connecting r and  $\sigma$  is used in preference to Stever & Rathbun's<sup>(15)</sup>, mainly because of its simplicity. It is

$$\sigma = \frac{\sigma_\infty}{1 + \frac{2\delta}{r}} \quad \text{or} \quad \sigma = \frac{r\sigma_\infty}{r+2\delta}$$

where  $\delta$  is some constant varying between 0.25 and 0.5 times the molecular diameter and subscript  $\infty$  refers to conditions at equilibrium over a plane surface.

Substituting this into the expression for critical droplet size above gives

$$r_* = \frac{2v_1}{kT \cdot \log_e (p/p_\infty)} \cdot \frac{r_* \sigma_\infty}{(r_* + 2\delta)}$$

which, on rearranging becomes

$$r_* = \frac{2v_1 \sigma_\infty}{kT \log_e (p/p_\infty)} - 2\delta$$

Differentiating the expression for surface tension above with respect to  $r$  gives

$$\frac{d\sigma}{dr} = \frac{2\delta\sigma_\infty}{(r+2\delta)^2} \quad \text{Similarly } \int_0^{r_*} r_* \cdot \sigma \cdot dr_* \quad \text{becomes on substitution } \sigma_\infty \int_0^{r_*} \frac{r_*^2 dr}{r_*+2\delta}$$

$$\text{which on integration gives } \sigma_\infty \left\{ \frac{r_*^2}{2} - 2\delta r_* + 4\delta^2 \log_e \left[ \frac{r_*+2\delta}{2\delta} \right] \right\}$$

This may now be substituted into the expression for rate of formation of nuclei giving

$$J = v_1 \left[ \frac{p}{kT} \right]^2 \left[ \frac{2}{\pi m} \right]^{\frac{1}{2}} \left[ \frac{\sigma_\infty r_*}{r_*+2\delta} - \frac{r_*^2 \delta \sigma_\infty}{(r_*+2\delta)^2} \right] \exp. B.$$

$$\text{where B now} = - \frac{8\pi}{kT} \left[ \sigma_\infty \left\{ \frac{r_*^2}{2} - 2\delta r_* + 4\delta^2 \log_e \left( \frac{r_*+2\delta}{2\delta} \right) \right\} - \frac{1}{3} \cdot \frac{r_*^3 \sigma_\infty}{(r_*+2\delta)} \right]$$

which further reduces to

$$J = v_1 \left[ \frac{p}{kT} \right]^2 \left[ \frac{2\sigma_\infty}{\pi m} \right]^{\frac{1}{2}} \frac{r_*}{(r_*+2\delta)} \exp. B. \quad \text{_____ (1)}$$

$$\text{with B} = - \frac{8\pi\sigma_\infty}{kT} \left[ \frac{r_*}{6(r_*+2\delta)} \left\{ r_*^2 - 6\delta r_* + 24\delta^2 \right\} + 4\delta^2 \log_e \left( \frac{r_*+2\delta}{2\delta} \right) \right]$$

$$\text{and with } r_* \text{ is given by } r_* = \frac{2v_1 \sigma_\infty}{kT \log_e(p/p_\infty)} - 2\delta \quad \text{_____ (2)}$$

TABLE 1.

Conditions at the collapse of supersaturation i.e. when = 0.1%								
Reservoir Conditions		Nozzle Geometry		Supercooling		Transit Time	Temp Grad.	Rate of Nuclei Formations
Press $P_0$ atm	Temp $T_0$ °K	Expansion Factor $K^2$	Throat Area $A_{t2}$ in	Mach No. $\Delta M$	Temp. $\Delta T$ °K	$\tau$ $10^{-6}$ secs.	$\frac{dT}{dx}$ °K/cm	J $10^{16}$ / cm <sup>3</sup> /sec
8.3	290	0.001	0.01	0.768	9.45	175.5	0.62	0.125
8.3	290	0.01536	0.01	0.938	11.25	56.4	2.05	7.88
8.3	290	0.03886	0.01	1.023	11.85	38.9	3.33	27.2
8.3	290	0.100	0.01	1.128	12.9	25.4	4.92	64.0
8.3	290	1.000	0.01	1.563	16.56	12.45	12.8	311.0
8.3	290	0.100	0.10	0.903	11.13	66.2	1.67	4.18
8.3	290	1.00	0.10	1.120	13.10	-	4.92	70.3
8.3	290	0.100	1.00	0.768	9.83	175.5	0.62	0.125
8.3	290	1.00	1.00	0.903	11.13	-	1.67	4.60
8.3	300	0.03886	0.01	1.088	12.85	-	2.94	24.6
8.3	310	0.03886	0.01	1.131	12.66	-	2.81	22.8
8.3	330	0.03886	0.01	1.233	13.48	-	2.38	20.2
8.3	450	0.03886	0.01	-	15.10*	-	-	-
8.3	380	0.03886	0.01	-	14.6*	-	-	-
10.0	310	0.03886	0.01	1.061	12.22	-	3.05	227.0
10.0	360	0.03886	0.01	1.338	12.95	-	1.63	175.0
16.0	290	0.03886	0.005	0.887	10.85	22.0	5.73	53.2
16.0	290	0.03886	0.010	0.838	10.66	29.6	4.35	2.09
16.0	290	0.03886	0.100	0.712	9.10	78.2	3.69	0.475
16.0	290	0.03886	1.00	0.628	8.17	202.6	4.01	0.00693
40.0	310	0.03886	0.01	0.685	10.06	-	6.53	83.8
40.0	360	0.03886	0.01	0.865	10.68	-	3.99	123.0
40.0	450	0.03886	0.01	-	11.75*	-	-	-
50.0	290	0.03886	0.01	0.583	7.83	-	8.5	53.3
70	360	0.03886	0.01	0.728	9.95	-	5.38	66.2
70	450	0.03886	0.01	1.005	10.85	-	2.65	104.0
100	290	0.03886	0.01	0.488	8.80	-	10.90	14.86

\* values obtained by extrapolation

TABLE 2.

Summary of parallel duct results.

VALUE.	Area Ratio $A/A_T$	Amount Condensed $\alpha$ (%)	Super Cooling $\Delta T$ (C°)	Mach No. M	$\Delta$ M	Drop Density $10^{10}/c.c.$	Meandrop Radius $r$ (Å)
At End Of Nozzle	30.5284	$2.77 \times 10^{-6}$	9.0	5.2874	1.253	0	0
After Four Dias. of Duct	"	$4.006 \times 10^{-3}$	9.0	5.2874	1.253	-	-
	33.3079	$5.378 \times 10^{-4}$	10.15	5.4036	1.360	7.48	114.1
	"	0.16	9.65	5.3906	1.347	-	-
	35.0360	$4.480 \times 10^{-3}$	10.90	5.4711	1.437	29.00	144.5
	"	0.60	9.45	5.4629	1.355	-	-
	38.6260	$9.945 \times 10^{-2}$	12.00	5.5892	1.555	108.10	222.0
	"	2.50	6.38	5.2652	1.231	-	-
	41.7550	0.500	11.9	5.6324	1.0417	244.60	322.0
	"	4.50	2.9	5.1007	0.6100	-	-
	47.0227	1.8	10.3	5.5919	1.0296	244.60	457.0
	"	Saturated	Sat.	5.1014	0.5391	-	-

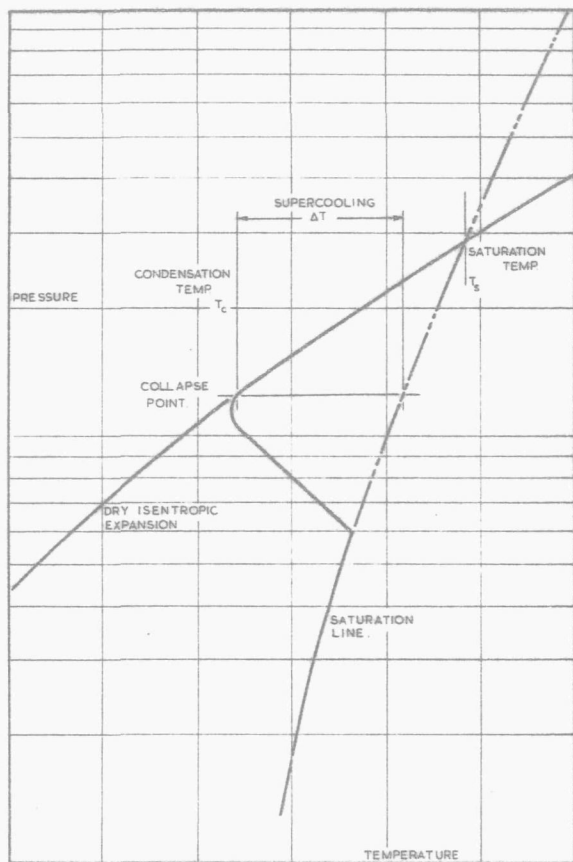


FIG. 1. THE COLLAPSE OF THE SUPERSATURATED STATE.  
(ON A TEMPERATURE PRESSURE DIAGRAM.)

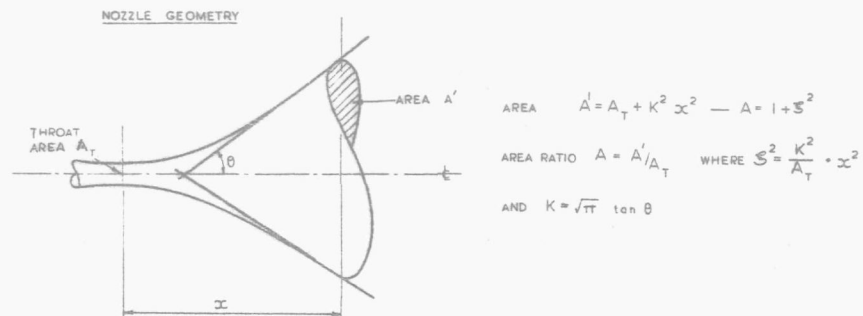


FIG. 2.

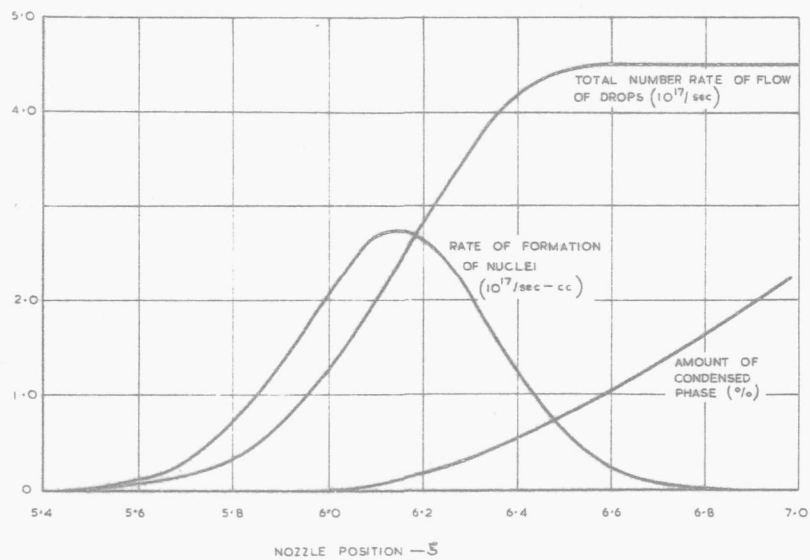


FIG. 3. TYPICAL VARIATION OF NUCLEI FORMATION RATE, TOTAL NUMBER RATE OF FLOW OF DROPS AND AMOUNT OF FLOW CONDENSED.

$$\left( \begin{array}{l} p_0 = 8.3 \text{ at m, } T_0 = 290 \text{ }^\circ\text{K} \\ A_T = 0.01 \text{ in}^2, K^2 = 0.03886 \end{array} \right)$$

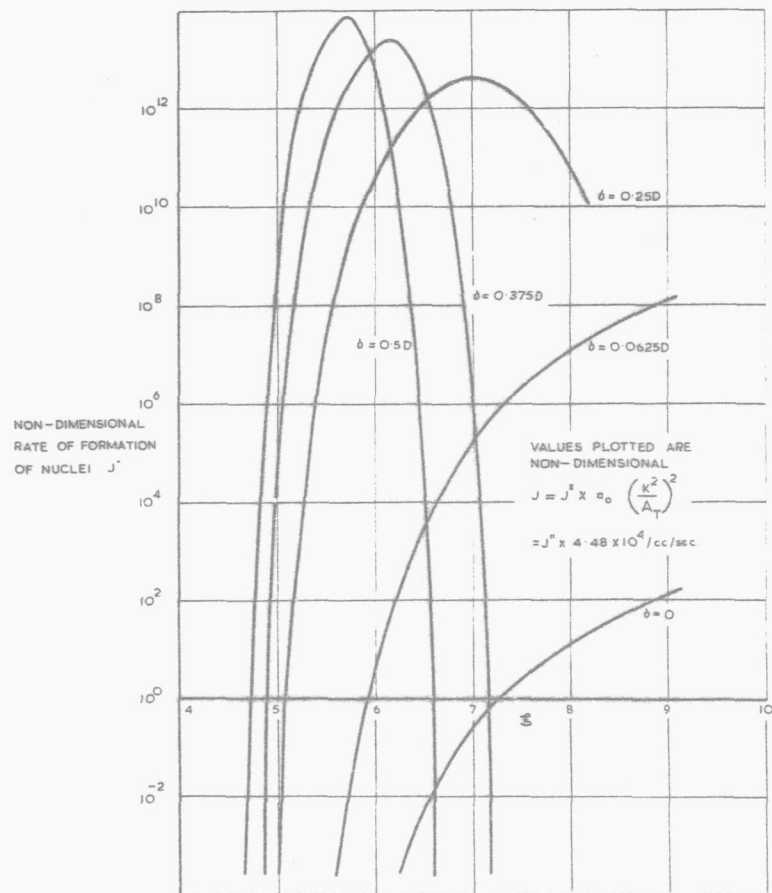


FIG. 4. EFFECT OF VARYING SURFACE TENSION ON NUCLEI FORMATION RATE.

$$\left( \begin{array}{l} p_0 = 8.3 \text{ atm. } T_0 = 290^\circ \text{K} \\ A_T = 0.01 \text{ in}^2, K^2 = 0.03886 \end{array} \right)$$

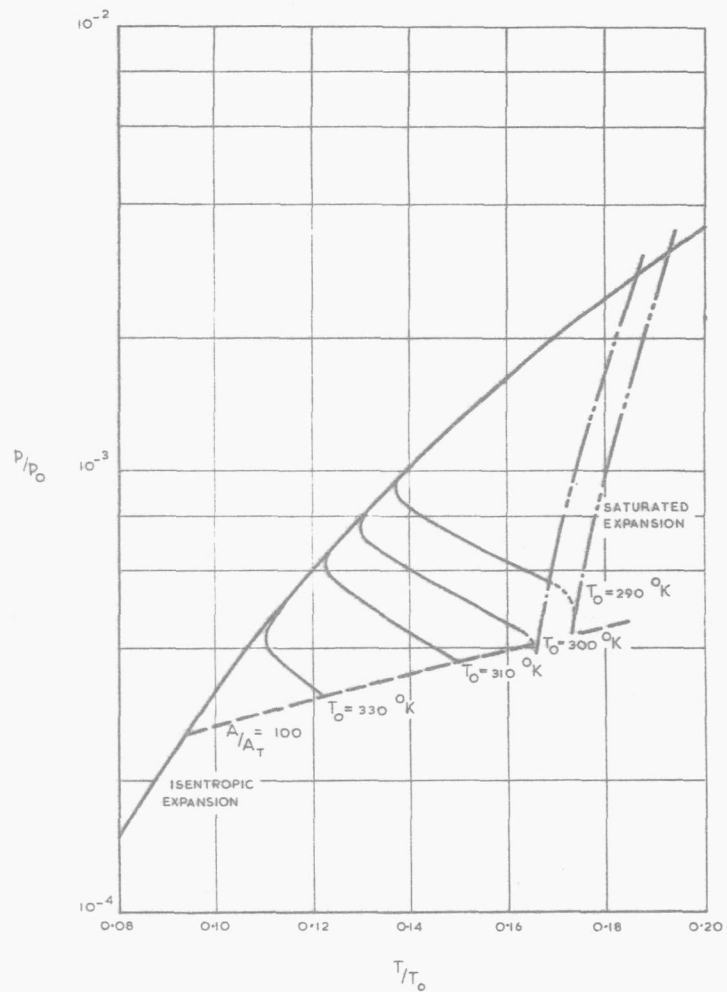


FIG. 5. THE COLLAPSE OF THE SUPERSATURATED STATE. THE EFFECT OF VARYING RESERVOIR TEMPERATURE.

$$\left( p_0 = 8.3 \text{ atm, } A_T = 0.01 \text{ in}^2, K^2 = 0.03886. \right)$$

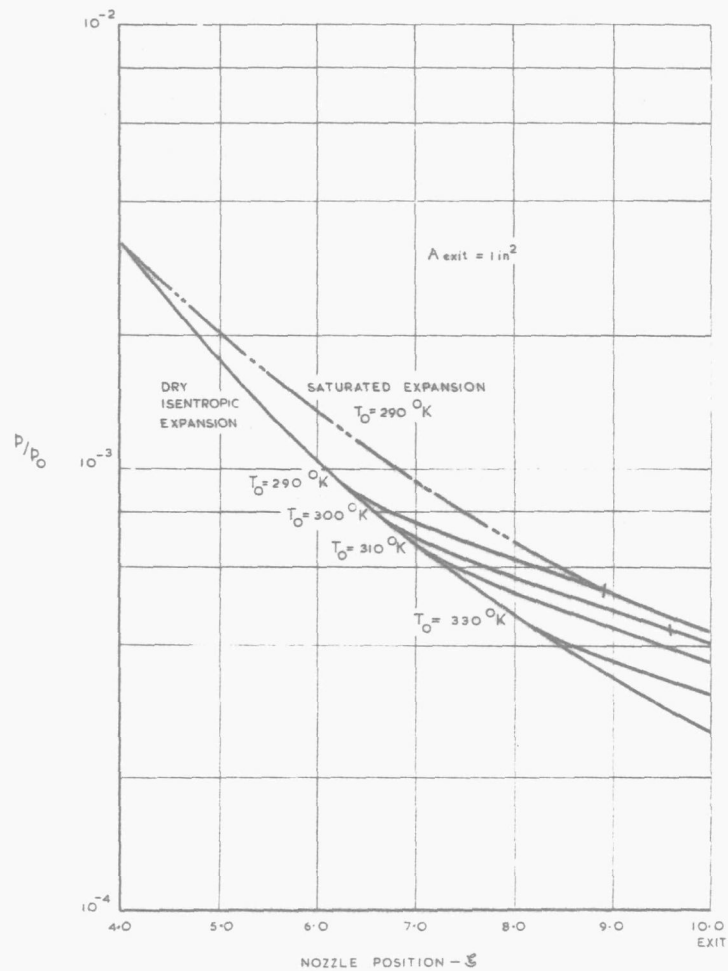


FIG. 5. THE EFFECT OF VARYING RESERVOIR TEMPERATURE ON THE NOZZLE PRESSURE DISTRIBUTION.  
 ( $p_0 = 8.3 \text{ atm}$ ,  $A_T = 0.01 \text{ in}^2$ ,  $K^2 = 0.03886$ )

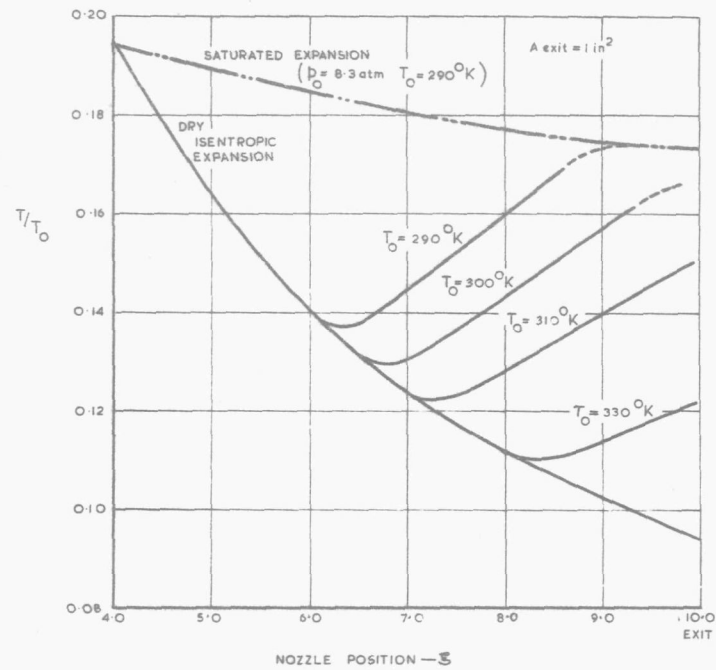


FIG. 7. THE EFFECT OF VARYING RESERVOIR TEMPERATURE ON TEMPERATURE DISTRIBUTION.  
 ( $p_0 = 8.3 \text{ atm}$ ,  $A_T = 0.01 \text{ in}^2$ ,  $K^2 = 0.03886$ )

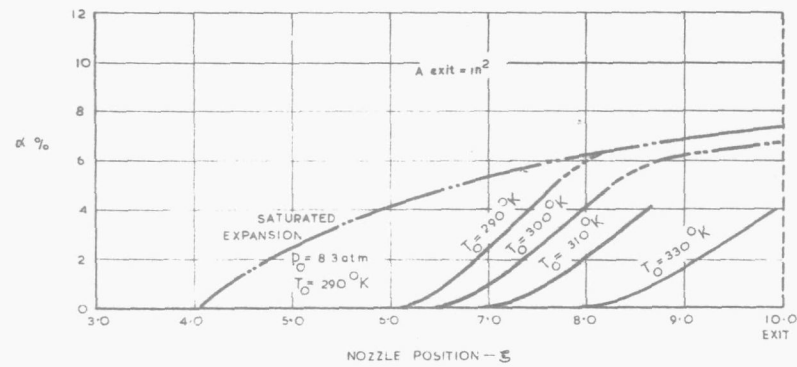


FIG. 8. THE EFFECT OF VARYING RESERVOIR TEMPERATURE ON THE AMOUNT OF FLOW CONDENSED.  
 ( $p_0 = 8.3 \text{ atm}$ ,  $A_T = 0.01 \text{ in}^2$ ,  $K^2 = 0.03886$ )

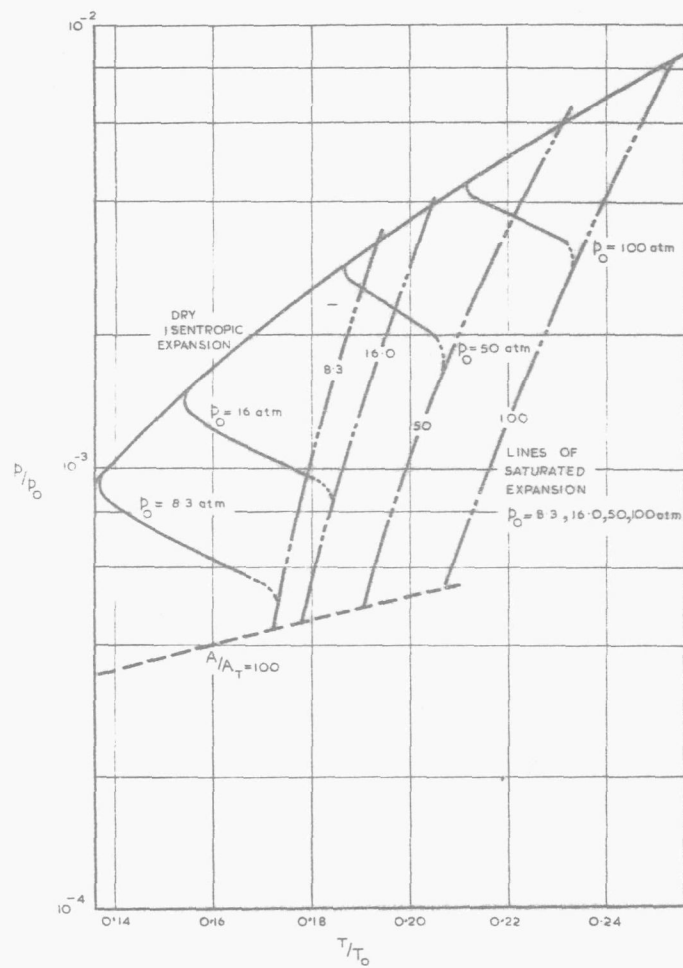


FIG.9. THE EFFECT OF VARYING RESERVOIR PRESSURE ON COLLAPSE.

( $T_0 = 290^\circ\text{K}$ ,  $A_T = 0.01$  in<sup>2</sup>,  $K^2 = 0.03886$ )

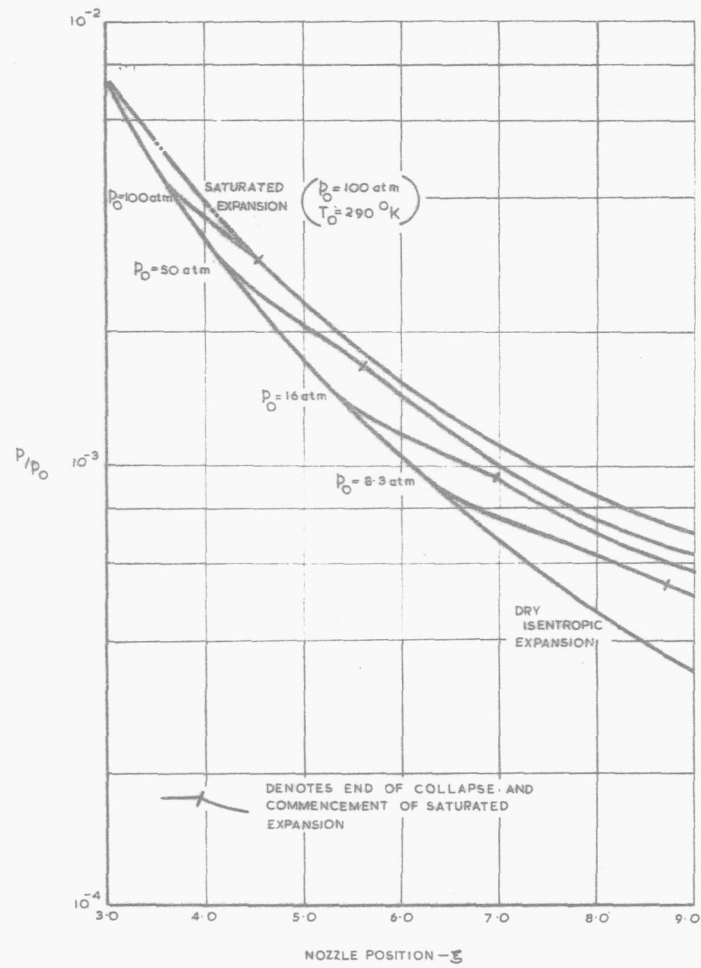


FIG.10. THE EFFECT OF VARYING RESERVOIR PRESSURE ON PRESSURE DISTRIBUTION.

( $T_0 = 290^\circ\text{K}$ ,  $A_T = 0.01$  in<sup>2</sup>,  $K^2 = 0.03886$ .)

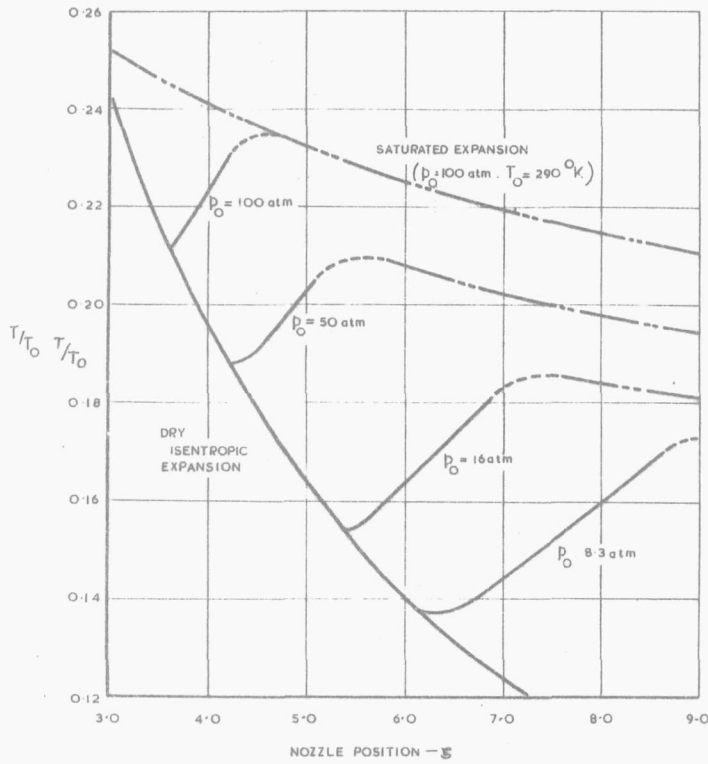


FIG.11. THE EFFECT OF VARYING RESERVOIR PRESSURE ON TEMPERATURE DISTRIBUTION.

$$(T_0 = 290^\circ \text{K}, A_T = 0.01 \text{ in}^2, K^2 = 0.03886)$$

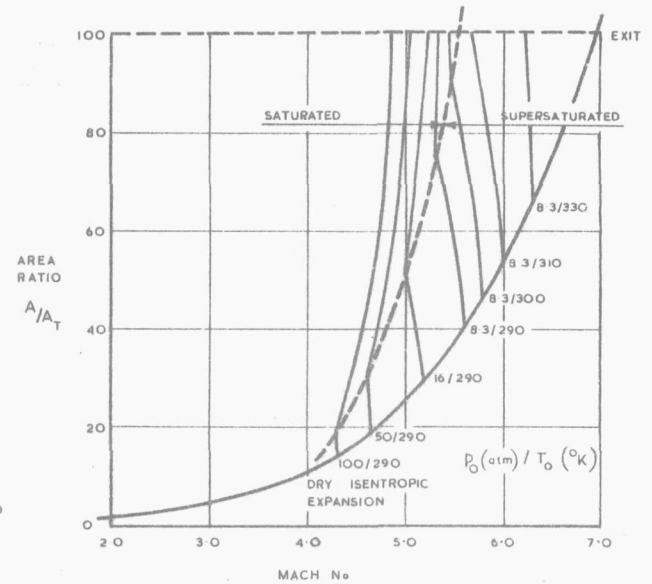


FIG.13. THE EFFECT OF VARYING RESERVOIR TEMPERATURE AND PRESSURE ON THE MACH No IN THE CONDENSING FLOW.

$$(A_T = 0.01 \text{ in}^2, K^2 = 0.03886)$$

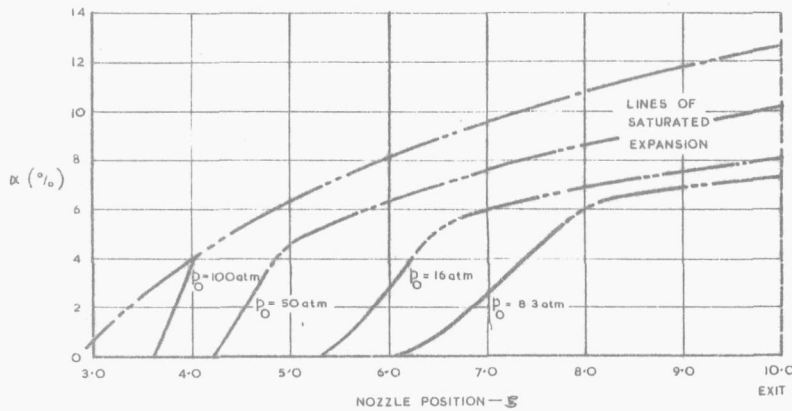


FIG.12. THE EFFECT OF VARYING RESERVOIR PRESSURE ON THE AMOUNT OF FLOW CONDENSED.

$$(T_0 = 290^\circ \text{K}, A_T = 0.01 \text{ in}^2, K^2 = 0.03886)$$

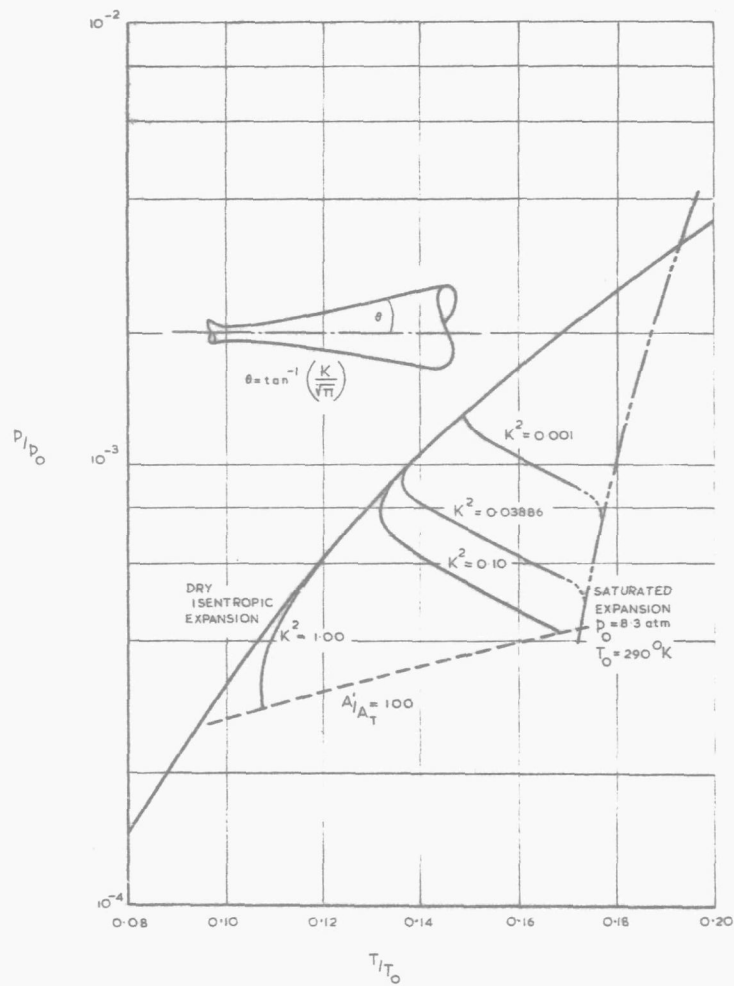


FIG. 14. THE EFFECT OF VARYING NOZZLE EXPANSION ANGLE ON COLLAPSE.

$$(p_0 = 8.3 \text{ atm}, T_0 = 290^\circ \text{K}, A_T = 0.01 \text{ in}^2)$$

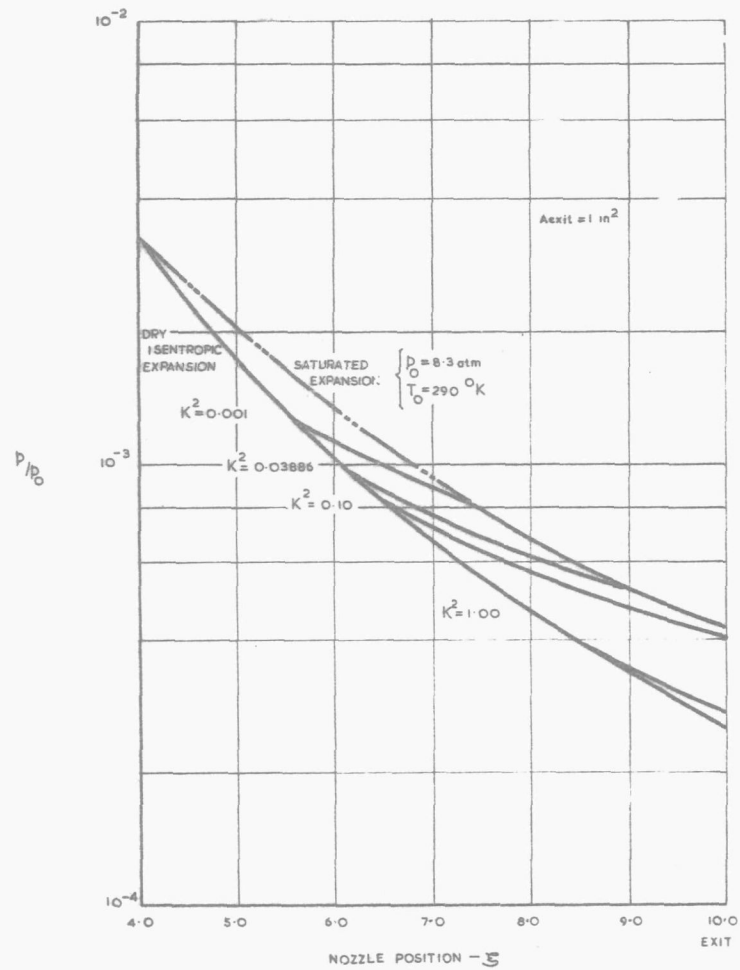


FIG. 15. THE EFFECT OF VARYING NOZZLE EXPANSION ANGLE ON PRESSURE DISTRIBUTION.

$$(p_0 = 8.3 \text{ atm}, T_0 = 290^\circ \text{K}, A_T = 0.01 \text{ in}^2)$$

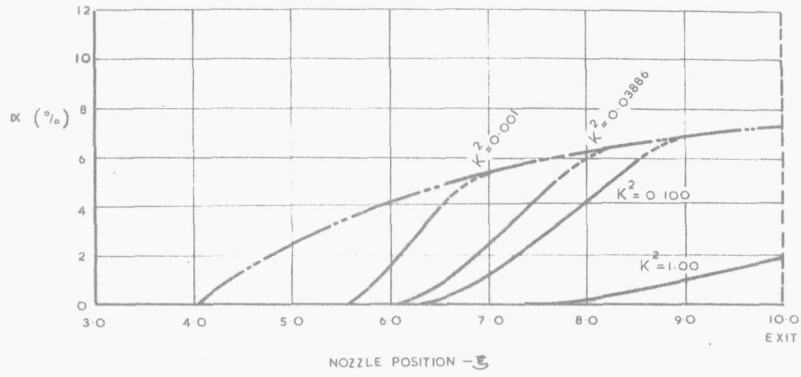


FIG. 16. THE EFFECT OF VARYING NOZZLE EXPANSION ANGLE ON THE AMOUNT OF FLOW CONDENSED.

$$(p_0 = 8.3 \text{ atm. } T_0 = 290^\circ \text{K. } A_T = 0.01 \text{ in}^2)$$

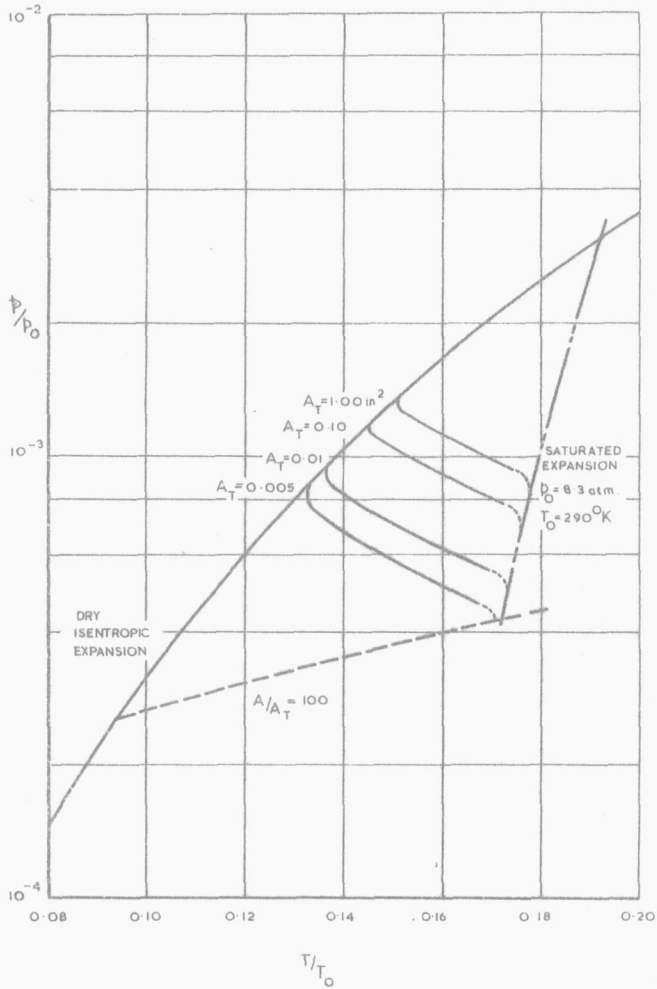


FIG. 17. THE EFFECT OF VARYING THROAT AREA ON COLLAPSE. ( $p_0 = 8.3 \text{ atm. } T_0 = 290^\circ \text{K. } K^2 = 0.03886$ .)

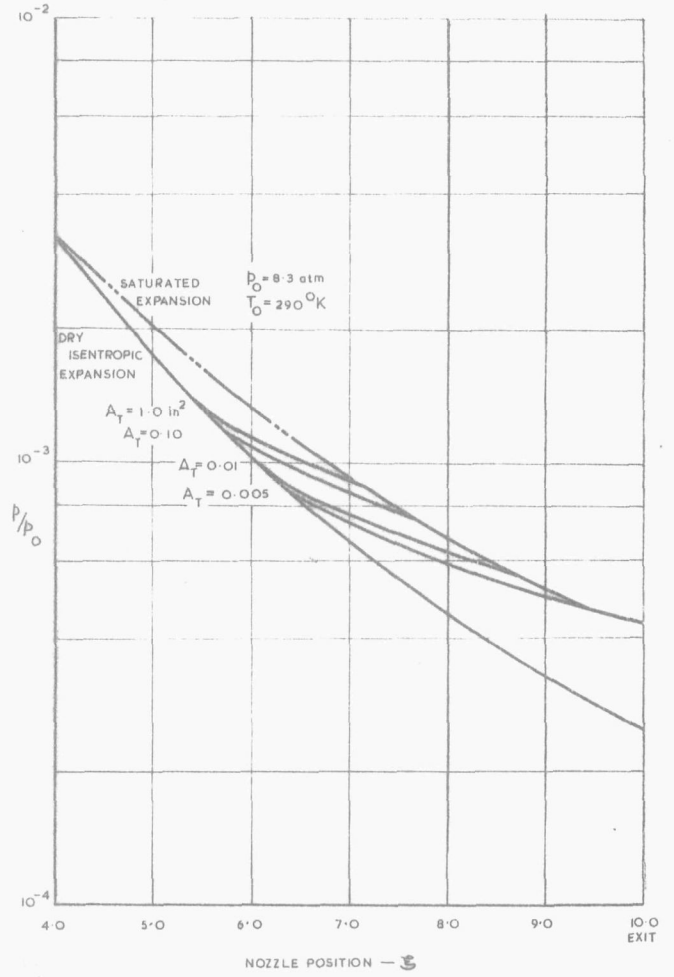


FIG. 18. THE EFFECT OF VARYING THROAT AREA ON PRESSURE DISTRIBUTION.

$$(p_0 = 8.3 \text{ atm. } T_0 = 290^\circ \text{K. } K^2 = 0.03886)$$

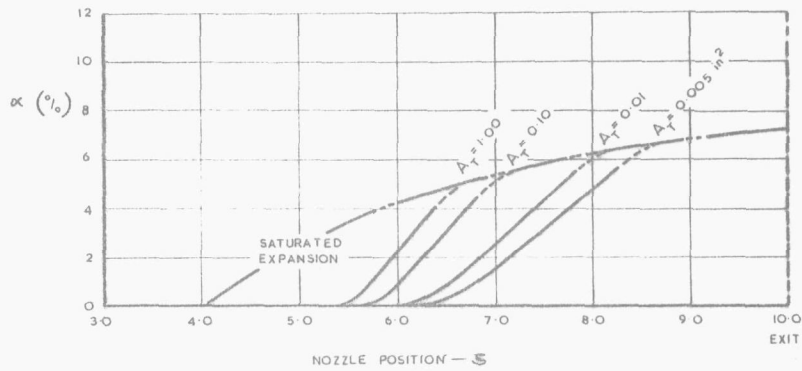


FIG. 19. THE EFFECT OF VARYING THROAT AREA ON THE AMOUNT OF FLOW CONDENSED.

( $p_0 = 8.3 \text{ atm}$ ,  $T_0 = 290^\circ\text{K}$ ,  $K^2 = 0.03886$ .)

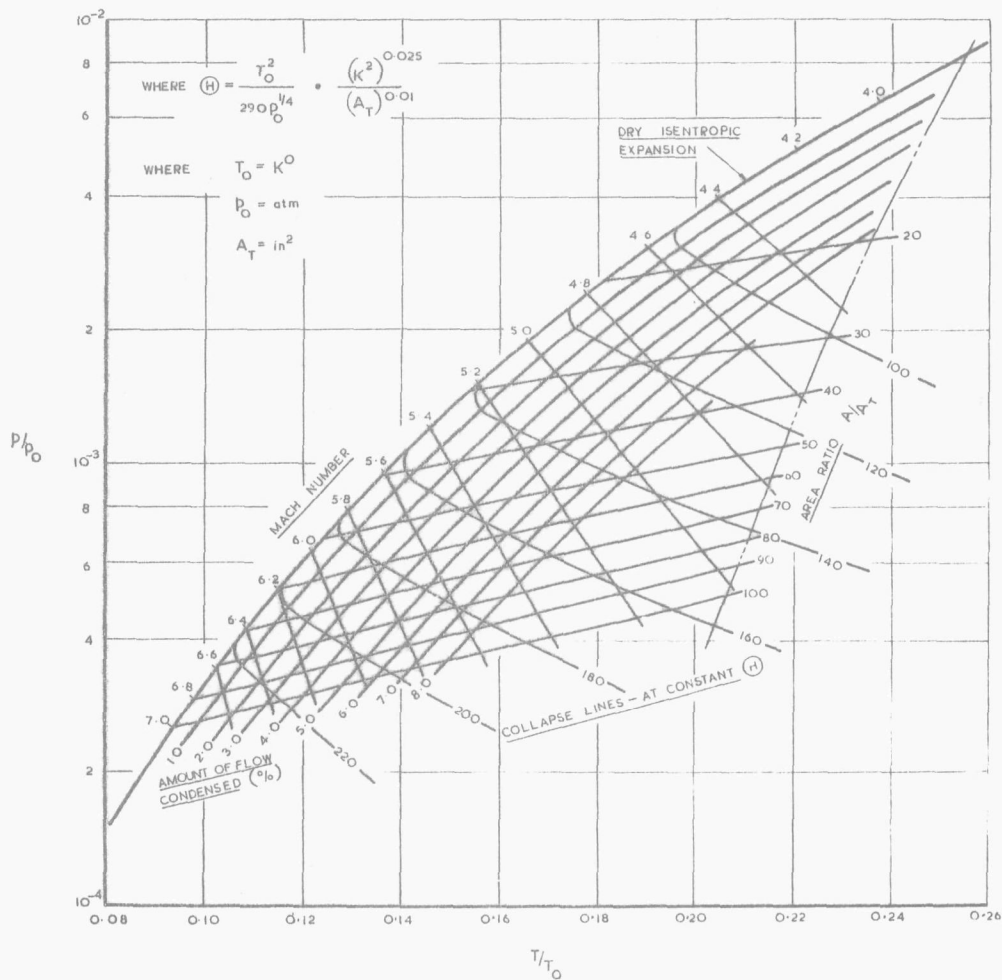


FIG. 20. CHART FOR THE ANALYSIS OF CONDENSING FLOWS OF SUPERSATURATED NITROGEN.

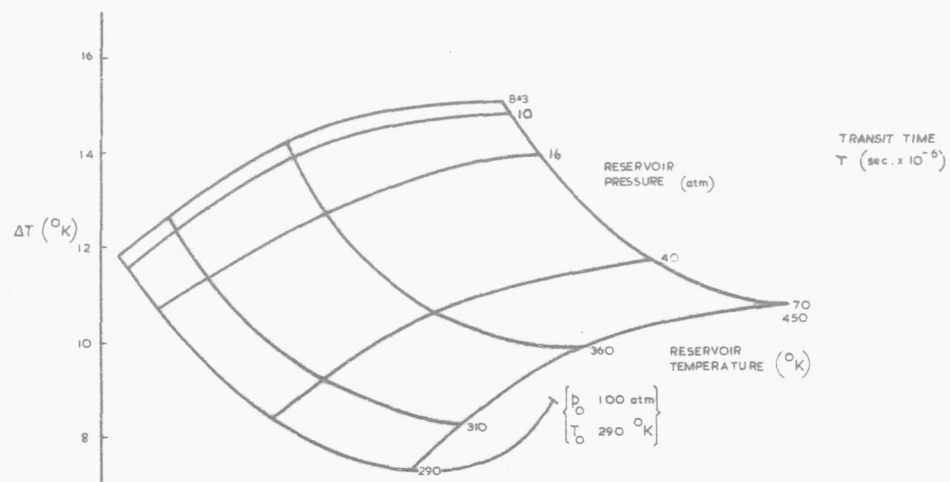


FIG. 21. THE EFFECT OF VARYING RESERVOIR CONDITIONS ON SUPERCOOLING WITH CONSTANT NOZZLE GEOMETRY.

$$(A_t = 0.01 \text{ in}^2, K^2 = 0.03886)$$

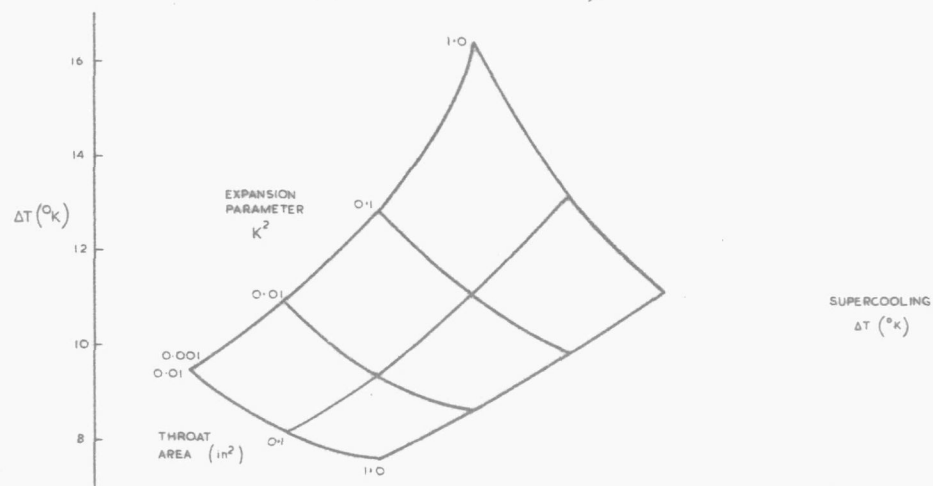


FIG. 22. THE EFFECT OF VARYING NOZZLE GEOMETRY ON SUPERCOOLING WITH CONSTANT RESERVOIR CONDITIONS.

$$(p_0 = 8.3 \text{ atm}, T_0 = 290^\circ\text{K})$$

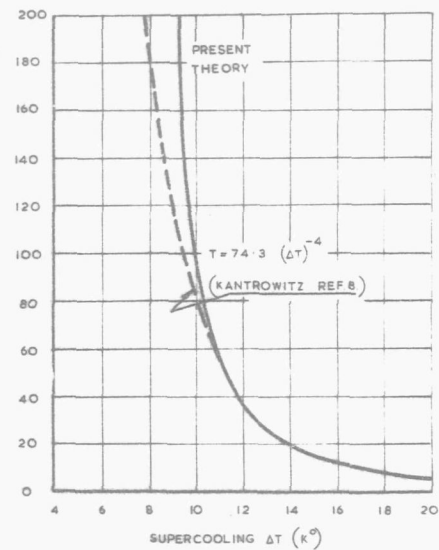


FIG. 23. THE VARIATION OF TRANSIT TIME (FROM SATURATION TO CONDENSATION) WITH SUPERCOOLING.  
( $p_0 = 8.3 \text{ atm}, T_0 = 290^\circ\text{K}, \text{ VARIABLE GEOMETRY.}$ )

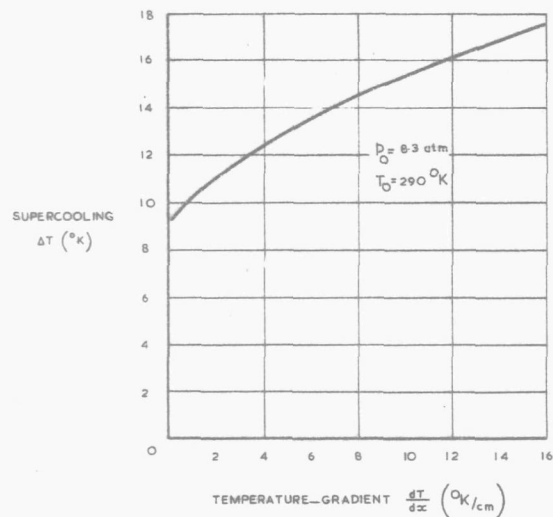


FIG. 24. THE VARIATION OF TEMPERATURE GRADIENT, PRIOR TO COLLAPSE, WITH SUPERCOOLING.  
( $p_0 = 8.3 \text{ atm}, T_0 = 290^\circ\text{K}, \text{ VARIABLE GEOMETRY.}$ )

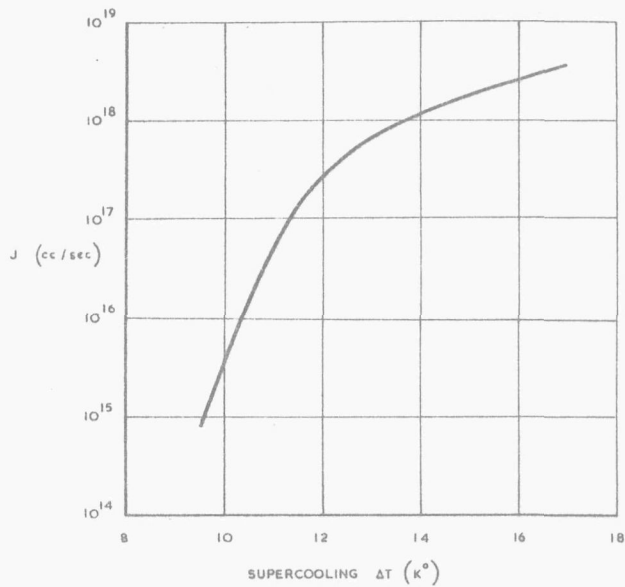


FIG. 25. THE VARIATION OF NUCLEI FORMATION RATE WITH SUPERCOOLING.  
 ( $p_0 = 8.3 \text{ atm}$ ,  $T_0 = 290^{\circ}\text{K}$  VARIABLE GEOMETRY)

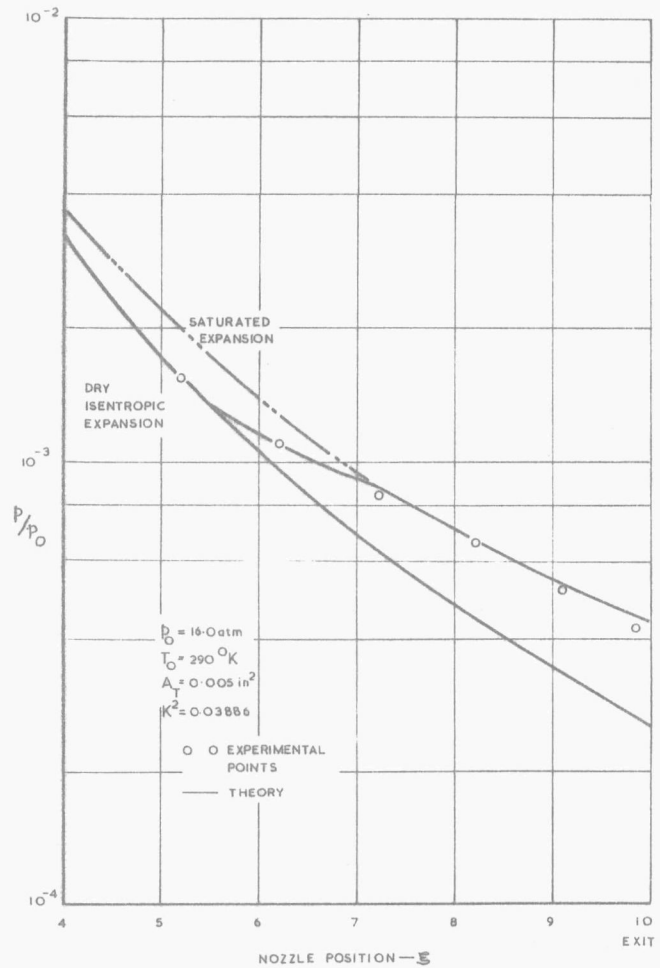


FIG. 27. PRESSURE DISTRIBUTION COMPARISON WITH EXPERIMENT — REF. 16. RUN. 13-2.

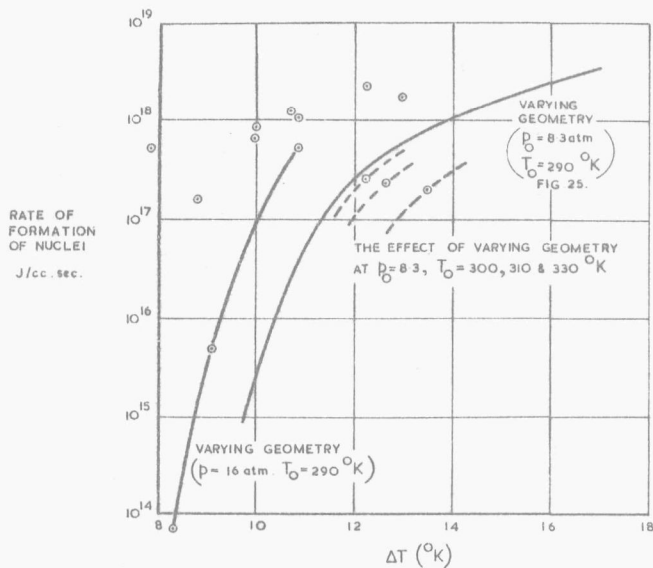


FIG. 26. THE RATE OF FORMATION OF NUCLEI FOR ALL CASES.

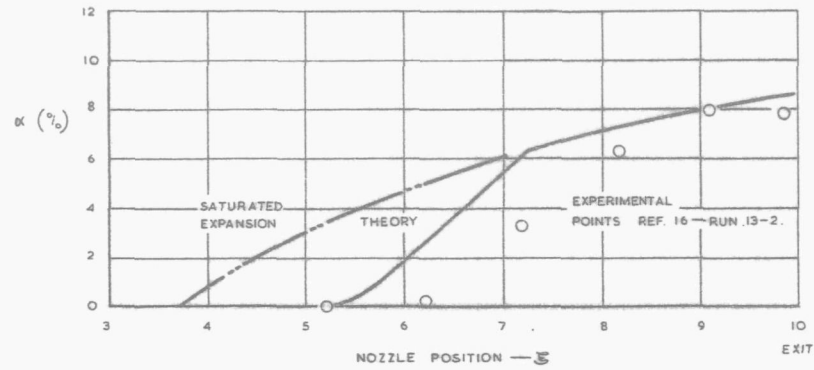


FIG. 28. AMOUNT OF CONDENSATE PRESENT. COMPARISON WITH REF. 16. RUN 13-2.

$$\left( \begin{array}{l} p_0 = 16 \text{ atm. } T_0 = 290 \text{ }^\circ\text{K} \\ A_1 = 0.005 \text{ in}^2. K^2 = 0.03886. \end{array} \right)$$

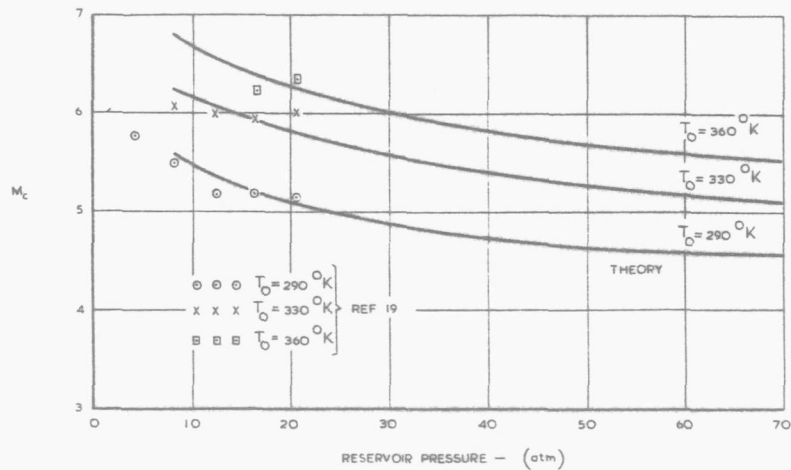


FIG. 30. THE EFFECT OF RESERVOIR CONDITIONS ON CONDENSATION MACH No. COMPARISON WITH EXPERIMENT REF, 19.

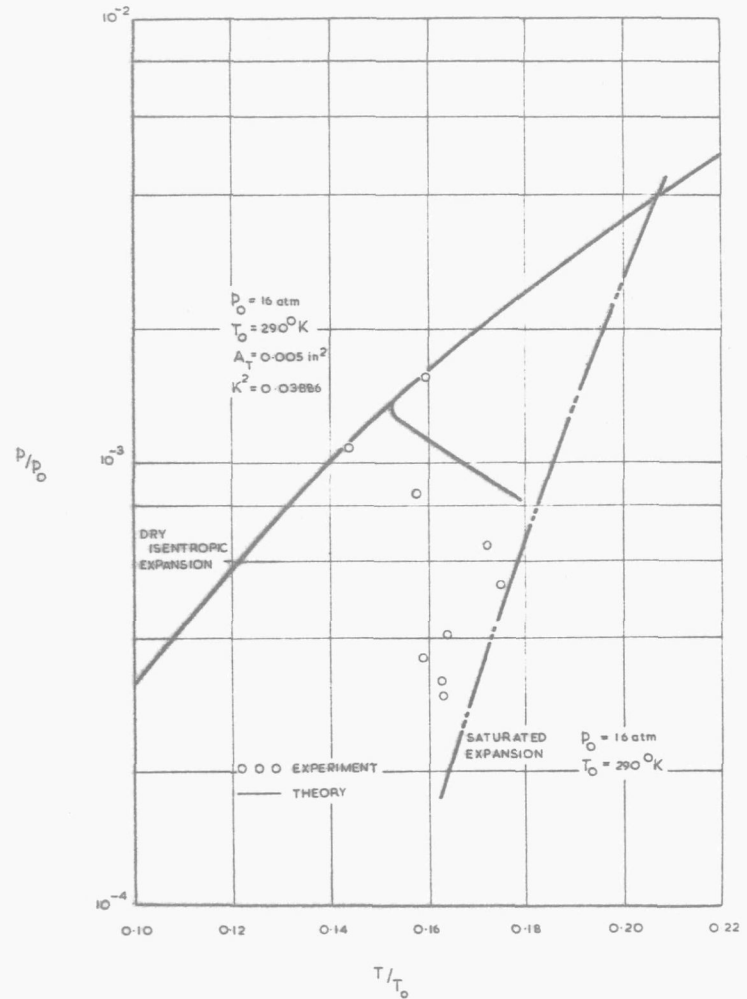


FIG. 29. THE COLLAPSE OF THE SUPERSATURATED STATE COMPARISON WITH REF. 16. RUN 13-2.

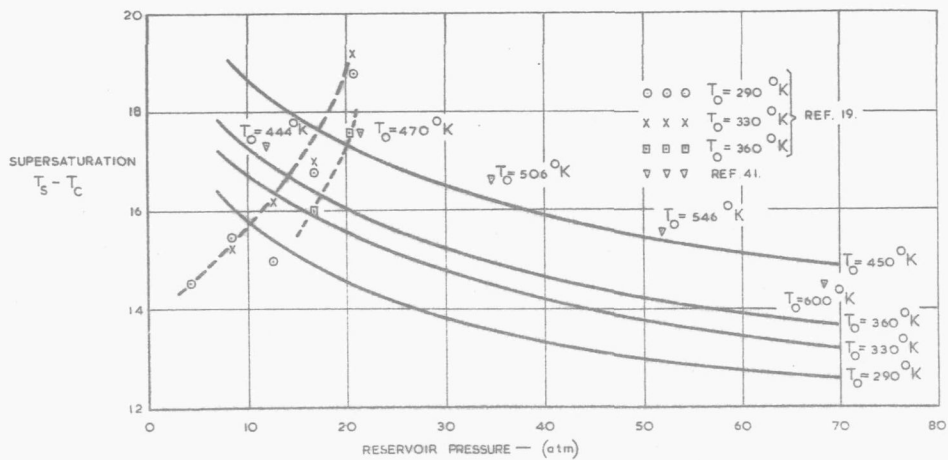


FIG. 31. THE EFFECT OF VARYING RESERVOIR CONDITIONS ON SUPERSATURATION COMPARISON WITH EXPERIMENT.

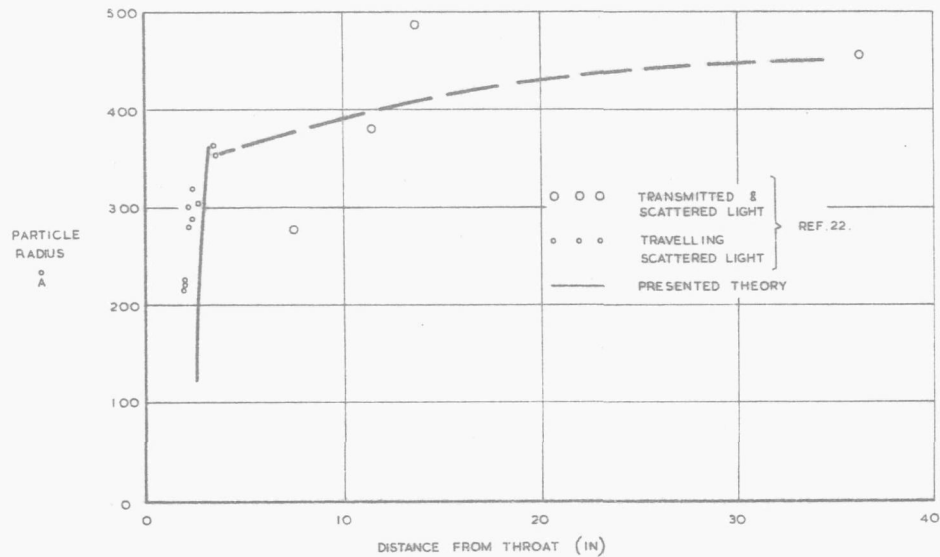


FIG. 33. PARTICLE SIZES. COMPARISON WITH EXPERIMENT, REF. 22.

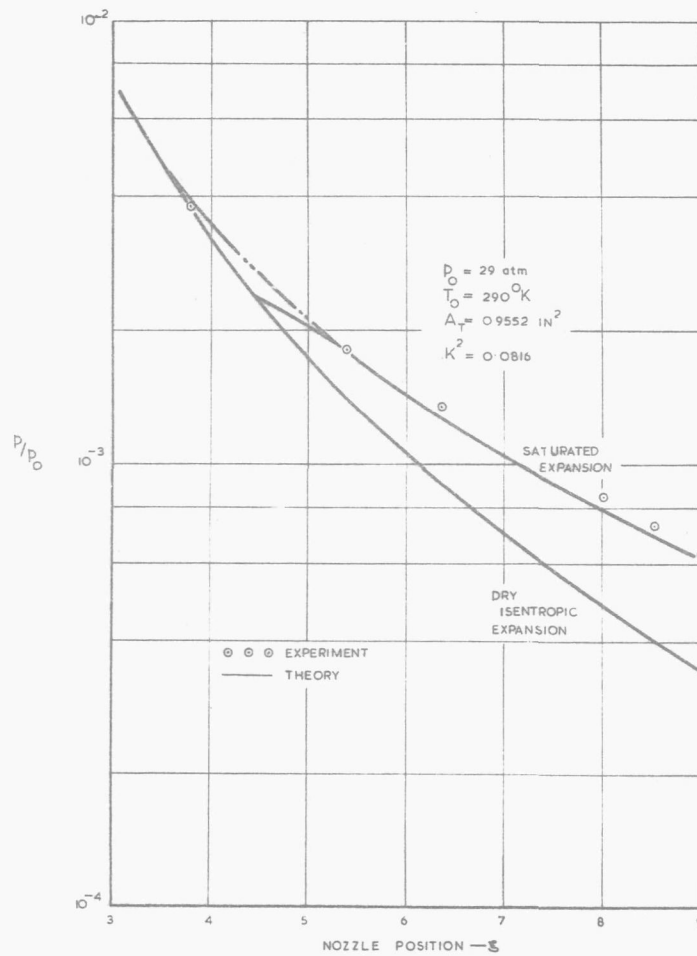


FIG. 32. COMPARISON WITH EXPERIMENT REF. 22. PRESSURE DISTRIBUTION.

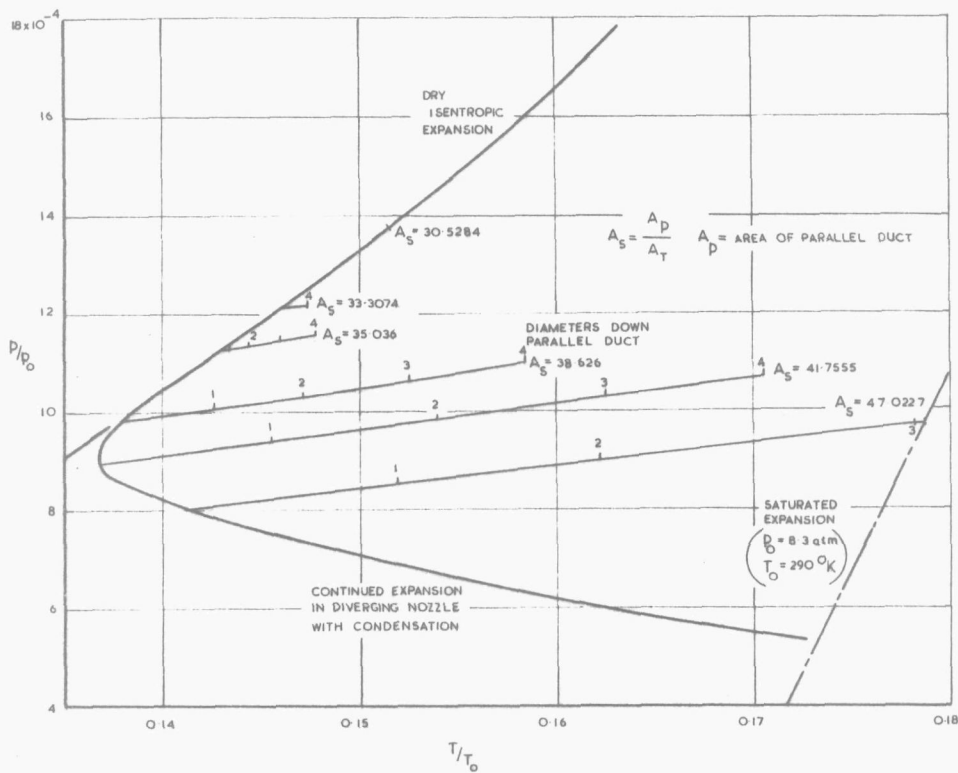


FIG. 34. THE COLLAPSE OF THE SUPERSATURATED STATE IN A NOZZLE FOLLOWED BY PARALLEL DUCT.

$$\left( \begin{array}{l} p_0 = 8.3 \text{ atm}, T_0 = 290^\circ \text{K} \\ A_T = 0.01 \text{ in}^2, K^2 = 0.03886 \end{array} \right)$$

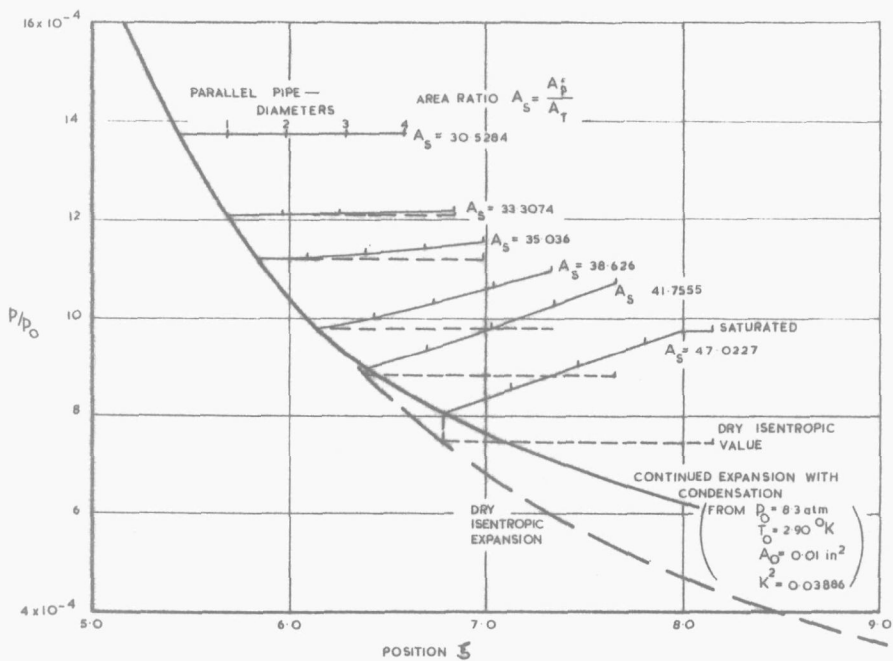


FIG. 35. EXPANSION OF SUPERSATURATED VAPOUR PRESSURE DISTRIBUTION IN NOZZLE FOLLOWED BY A PARALLEL DUCT.

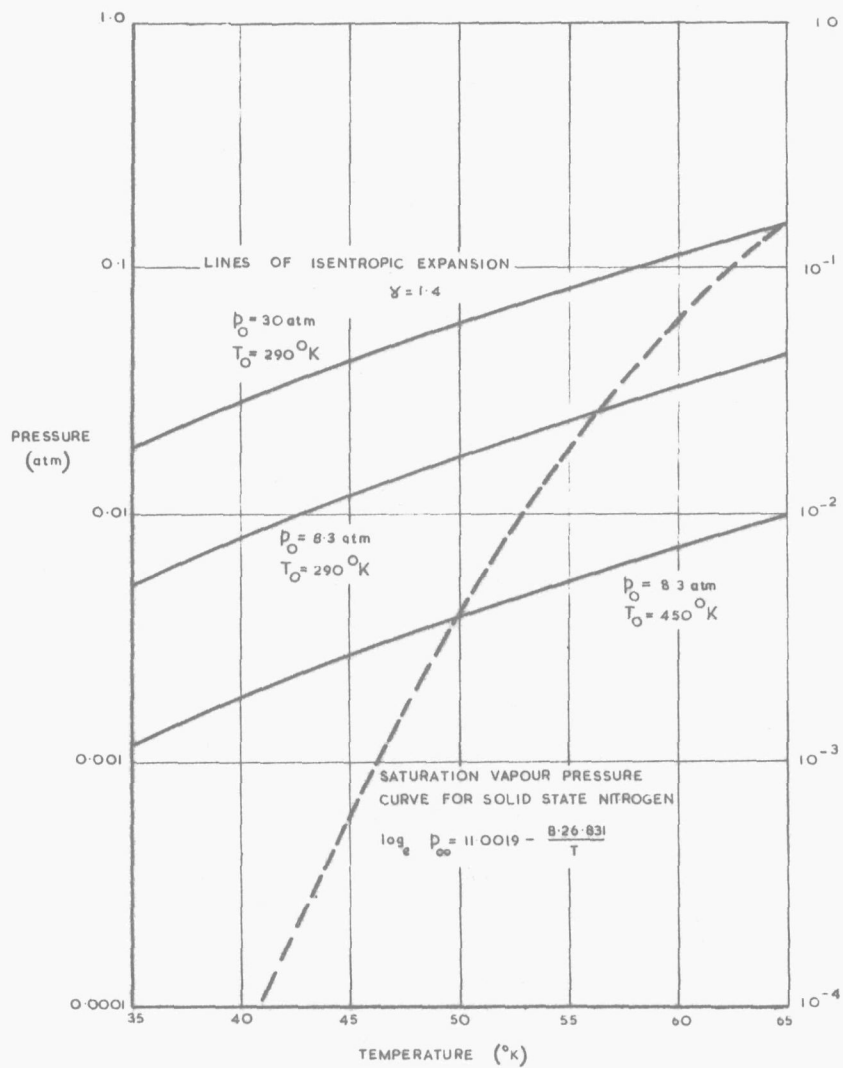


FIG. 36.